福岡工業大学大学院工学研究科

Surface Modification and Functionalization of Hexaniobate Nanosheets with DNA and Polymethylmethacrylate

DNAおよびポリメチルメタクリレートによる六ニオブ酸塩ナノシートの表面修飾と機能化

福岡工業大学大学院　博士後期課程工学研究科物質生産システム工学専攻
宮元研究室　安樂　信哉
指導教員　　宮元　展義

Chapter 1 Introduction
1.1General Introduction
1.2Layered crystal and nanosheets
1.2.1Layered crystals
1.2.2Nanosheet liquid crystal

1.3Surface modification of layered crystal and nanosheet
1.3.1Silylation
1.3.2Alcohols
1.3.3Phosphoric acid derivative
1.3.4Other modification species

1.4 Composite of DNA and nanosheet
1.4.1DNA
1.4.2DNA nanotechnology
1.4.3Composite of DNA and nanomaterials
1.4.4Composite of DNA and nanosheet

1.5Reference

Chapter 2 Grafting of Fluorescence-Labeled ssDNA onto Inorganic Nanosheets and Detection of a Target DNA
2.1Introduction
2.2Experiment
2.3Result and Discussion
2.4Conclusion
2.5Reference

Chapter 3 Modification of PMMA on to hexaniobate nanosheet colloid maintaining dispersed state in a mixture solvent of water/DMF
3.1Introduction
3.2Experiment
3.3Result and Discussion
3.4Conclusion
3.5Reference

Chapter 4 Conclusion

4.1 Conclusion
4.2Publication list
4.3Acknowledgments

Chapter 1

Introduction

1.1General Introduction

Inorganic nanosheets obtained by exfoliation of layered crystal are anisotropic colloidal particles with the thickness of 1 nm and the lateral size of several μm. Nanosheets have been investigated for the nanomodules to fabricate functional nanomaterials such as electronics device based on multi-layered nanofilms, high performance nanosheet/polymer composite materials, and soft materials with liquid crystallinity and structural color. Due to huge surface area, nanosheets are also important in the applications for adsorbent, catalyst and sensor. To further widen the range of applications such as adsorbent with high selectivity and tough nanocomposites with hydrophobic polymer, grafting of functional molecule on nanosheet surfaces is very important. In conventional studies, the interlayer surfaces of the layered crystal were grafted, followed by partial exfoliation; however, only low degree of exfoliation was achieved and modifying with bulky species was difficult. In this thesis, a functional biomolecule, ssDNA, and a synthetic polymer, methylmethacrylate, was successfully modified on hexaniobate nanosheet surface having hydroxyl group by originally developed method. This thesis is composed of 4 chapters as follows.

In the Chapter 1, background of this thesis is described. Nanosheet liquid crystal, modification of layered crystaland composites of DNA and nanosheet are reviewed.

In the Chapter 2, fluorescence-labeled ssDNAs were grafted on hexaniobate nanosheet. The fluorescence of the ssDNA-grafted nanosheet were quenched by adding complementary ssDNA with a quencher molecule, confirming that the grafted ssDNA can undergo hybridization reaction on the nanosheet surface. These results are important for future applications such as gene-therapy and fabrication nanocomposites by DNA-nanotechnology.

In the Chapter 3, hexaniobete nanosheets were successfully grafted with 3-(trimethoxysilyl)propylmethacrylate(MPDMS) by the silylation reaction maintaining the fully dispersed state of the nanosheets in solvent. Polymer-grafted nanosheet were then synthesized by polymerizing methylmethacrylate by radical polymerization stating from the grafted MPDMS. Polymer-grafted nanosheets were well-dispersed in organic solvents due to steric stabilizing effect, keeping liquid crystallinity. Based on the present material, mechanically tough nanosheet/hydrophobic polymer composites with precisely regulated structure will be developed.

In Chapter 4, conclusion of this thesis is shown.

1.2 Layered crystal and nanosheets

1.2.1 Layered crystals

Inorganic layered crystals such as graphene, layered clay minerals, and layered hexaniobate are the compounds in which many plate-like particles (nanosheets) are staked. There are various factors that affect the physical properties of the layered material itself, such as the composition of the layer , the composition and environment between layers, and the order of stacking. For example, kaolinite has an asymmetric layer, and it has been reported that the orientation of guest molecules is controlled by utilizing the asymmetry, showing the peculiarity of the two-dimensional nanospace. Layered hexaniobate is another interesting example: there are two types of alternating interlayer spaces and it has a photocatalytic function.

The surface of most of inorganic layered crystals is positively or negatively charged. Therefore, ions having a charge opposite to the surface charge of the layer compensate the layer charge. In this way, the layers of the inorganic layered crystal form a three-dimensional structure through electrostatic attraction or van der Waals force. Therefore, it is possible to break the bond between layers and take in different molecules or ions. This is called intercalation, and the compound produced by intercalation is called an intercalation compound. [1] Molecules or ions that are taken in the *host* inorganic layered crystal are called *guest* species (Figure1-1).

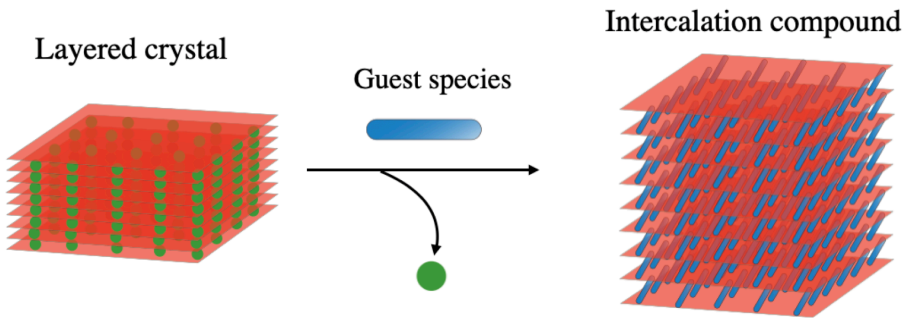

Figure 1-1 Intercalation reaction of layered crystal

Various molecules such as solvent molecules, ions, and macromolecules can be used for intercalations. Since intercalation is a reaction that combines different substances, a host and a guest, at the nanoscopic scale, it is useful for developing various functional materials with unique physical and chemical properties such as pillared clay,[2]polymer composite,[3] applicable for catalyst,[4] adsorbent.[5]

1.2.2 Nanosheet Liquid Crystal

As previously explained, many kinds of layered crystals with various composition, crystal structure and property are known. Intercalation compounds are generated by intercalation of guest species into interlayer of layered crystal. When many solvent molecules intercalate in interlayer of layered crystal, inorganic nanosheet is obtained by expansion of interlayer spacing due to swelling of layered crystal, followed by exfoliation of layer. The inorganic nanosheet is ultra-anisotropic particle having the thickness of ~1 nm and width of several μm . (Figure 1-2 and 1-3)

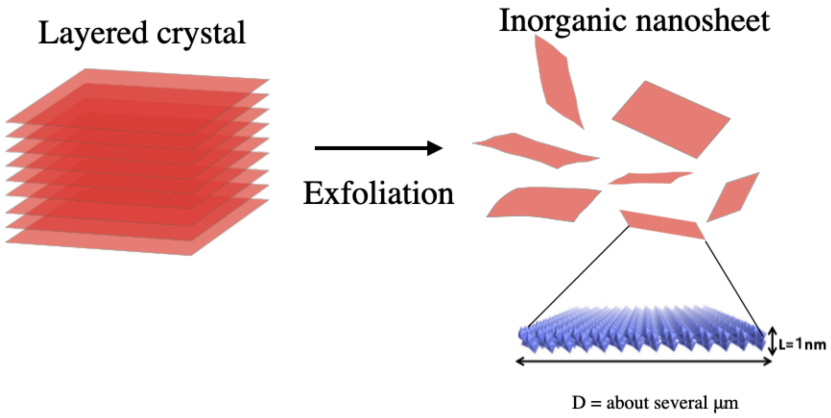

Figure 1-2 Exfoliation of layered crystal

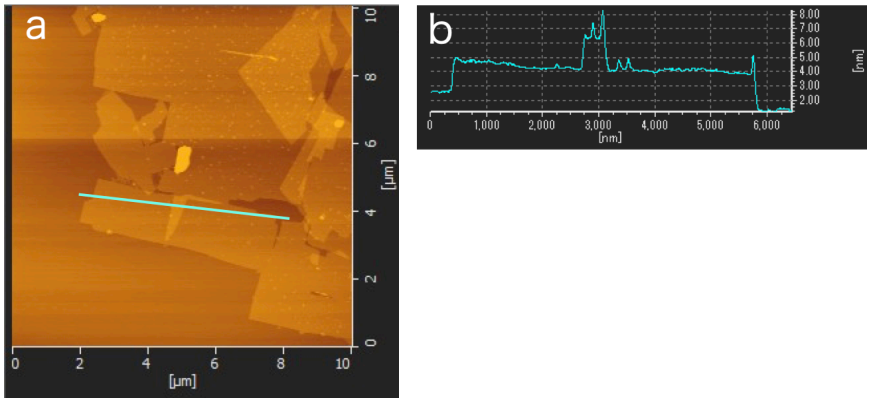

Figure 1-3 AFM image of (a) the hexaniobate nanosheet and (b) its cross section profile

A highly swelling smectite clay mineral exfoliates facilely just by addition of powder sample into water. However, in many cases of obtainment of nanosheet, original Ions of interlayer in the layered crystal need to exchange suitable ions such as tetrabutylammonium ion and *n*-propylammonium ion. By ions exchange, expansion of interlayer spacing of layered crystal due to increase of affinity of solvent molecules for

interlayer promotes swelling and exfoliation of interlayer. Inorganic nanosheet is characterized as 2D inorganic polymer electrolyte with highly negative charge or positive charge, diffusion layer of counter ions is formed around dispersed nanosheet and nanosheet colloid disperse stably in the solvent. Moreover, the nanosheet colloid dispersed in solvent is formed a liquid crystal phase due to autonomic orientation by increase of nanosheet concentration.(Figure 1-4)

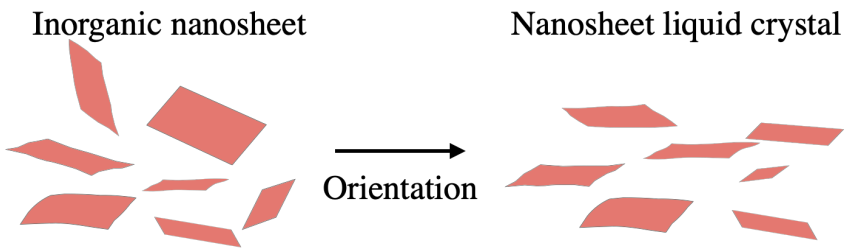

Figure 1-4 Formation of nanosheet liquid crystal

This liquid crystal is called *nanosheet liquid crystal* and have been studied as new type liquid crystal. Liquid crystal of expression of concentration change of anisotropic dispersed material like the nanosheet liquid crystal is called lyotropic liquid crystal which is known aqueous surfactant solvent, rigidity polymer solution like a DNA,[6] rod-like grain [7]and nano-platelet.[8] Nanosheet is interesting material due to a rare 2D particle in the lyotropic liquid crystal and marked anisotropic rate.

Many kinds of nanohseet liquid crystals such as layered phosphate($K_3Sb_3P_2O_{14}$[9], α-zirconium phosphate[10]), layered transition metal oxide($K_4Nb_6O_{17}$,[11] KTiNbO,[12] KNb_3O_8,[13] $H_{1.07}Ti_{1.73}O_4$,[14] $KCaNb_3O_{10}$[15]), layered clay mineral(montmorillonite, laponite, beidellite,[16], nontronite,[17] fluorohectorite[18]) and graphene oxide[19], [20]have been reported.

Liquid crystal nanosheet is expected as soft material to disperse in the solution, in addition of properties of layered crystal which are optical, magnetical and catalytic functions , two-dimensional organization of adsorbed guest molecules and surface modification. Functional materials with nanostructure such as multi-layered thin film,[21] porous substance[22] and inorganic/polymer hybrid[23] are obtained by using the nanosheet dispersed in solution. Understanding and control of liquid crystal structure of nanosheet is vitally significant for application due to by way of colloidal state dispersed nanosheet in a solution.

1.3 Surface modification of layered crystal and nanosheet

1.3.1 Silylation

While natures and interesting studies of layered crystal and nanosheet is introduced in the previous chapter, this section deals with grafting of organic species on the layer surface though covalent bond onto interlayer of layered crystal having a hydroxy group on the surface such as layered silicate and layered transition metal oxide. Modification of organic species onto layered crystal enables to change the property such as water repellency, corrosion resistance and heat-resistance on the surface. Focusing on the organic species modifying onto substrates, studies of modification onto layered crystal and nanosheet is explained comprehensively with classification of organic species into four categories: silane coupling agents, phosphoric acid derivations, alcohols and other modification species.

Silylation is the chemical reaction to graft silane coupling agents onto the hydroxy group of inorganic material surface; stable organic derivations of the material are expected through covalent bond. Also, silane coupling agents with various functional group are commercially available and suitable agents are chosen for desired purposes. Typical silylation reaction is shown in Figure 1-5,[24] and expressed as

$$\equiv Si - OH + XSiR_3 \rightarrow \equiv Si - O - SiR_3 + HX$$

Reactivity of silane coupling agents are different, depending on the reaction site (X groups : X = Cl, OMe, OEt) of number and types; Cl >> OMe > OEt. Uniform dispersion of silylated silica particles into polymer matrix and surface modification on the glass and silicone substrate have been researched actively.

Ruiz-Hitzky and Rojo[24]firstly reported modification of silane coupling agents (trimethylchlorosilane or hexamethyldisilazane) onto interlayer of H-type magadiite; the swelling of interlayer by intercalation of solvent molecules is important for the silylation. Ruiz-Hitzky et al.[25] also reported that intermediate expanded interlayer by intercalation of solvent molecules allowed the modification of small size of silane coupling agents, but not the modification of large size of silane coupling agents due to no intercalation of the silane coupling agent.

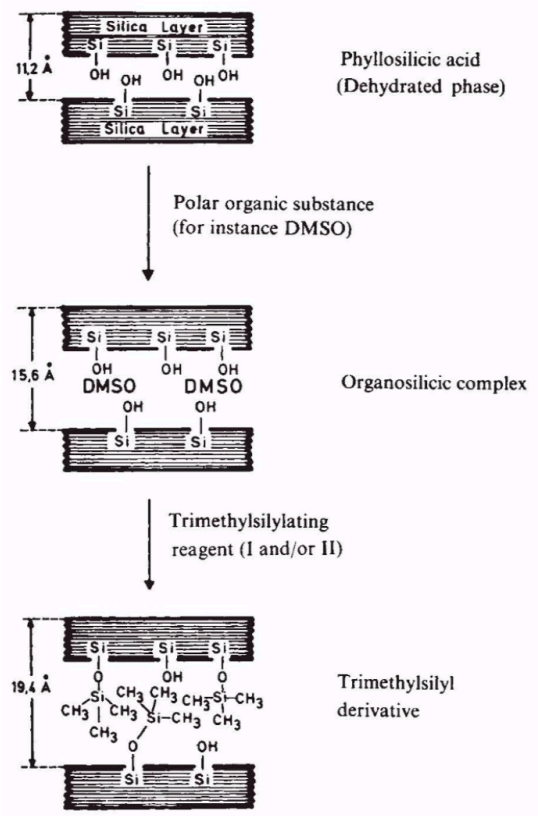

Figure 1-5 Schematic representation of the trimethylsilylation of layered polysilicate[24]

Yanagizawa et al. have reported the use of alkyltrimethylammoniumion intercalated magadiite and kenyaite for silylation.[5] (Figure 1-6) This silylation method allowed the modification of large size of silane coupling agents, and represented high modification rate than Ruiz-Hitzky's method. Yanagizawa's method has become a general method of modification of organic molecules onto interlayer of layered crystals. H-type magadiite was modified with various types of silane coupling agents such as hexamethyldisilazane,[5] allyldimetylchlorosilane,[26] alkyltrimethoxysilane,[27] 3-aminopropyltrimethylsilane,[28] 3-(2- aminoethylamino) propyltrimethoxysilane[29] and so on. Silylation was reported for modification of layered silicate other than magadiite such as kanemite,[30] octosilicate,[29],[31],[32],[33],[34-36] and a layered clay mineral.[27, 28, 37-42] Ide and Ogawa reported notable study on modification of two types of silane coupling agents onto the octosilicate.[35] Also, polymer modified montmorillonite was synthesized by modification of bis-bromo-triethoxysilane linker onto the edge of montmorillonite and polymerization of *N*-isopropylacrylamide onto bis-bromo-triethoxysilane linker modified

montmorillonite.[42](Figure 1-7)

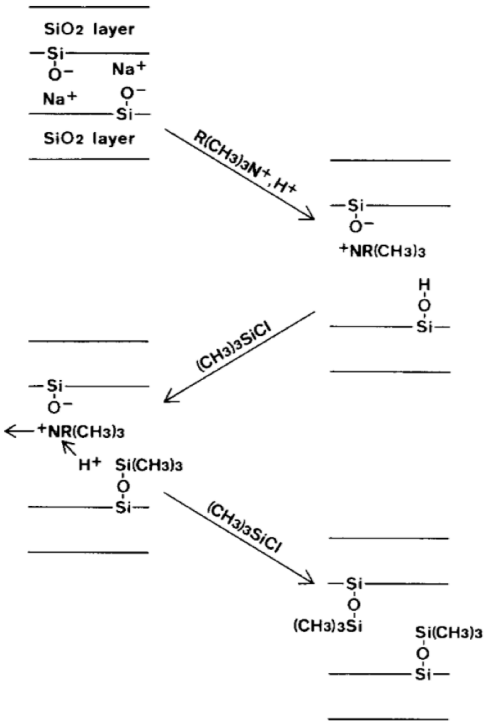

Figure 1-6 Schematic representation of trimethylsilylation of layered polysilicate (R = $C_{12}H_{25}$)[5]

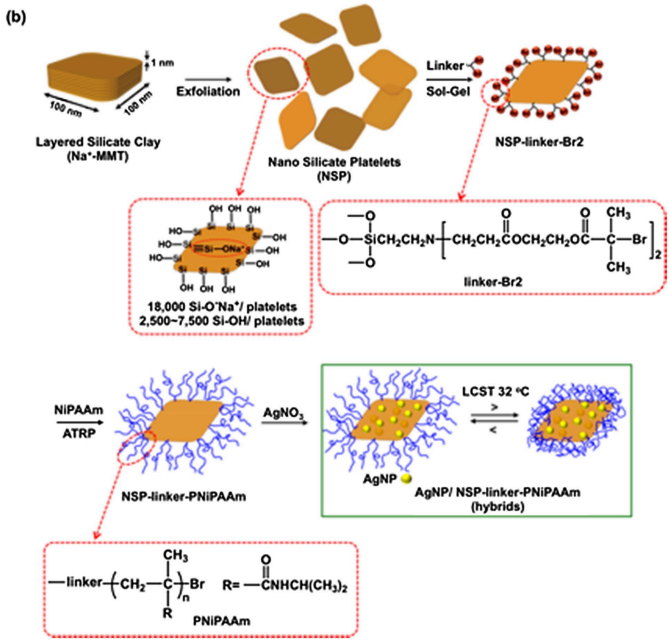

Figure 1-7 Conceptual diagrams of montmorillonite -PNiPAAm by ATRP and in-situ reduction of Ag^+ to Ag nanoparticles to afford the thermo-responsive Ag nanoparticle/ montmorillonite -PNiPAAm[42]

Following the many reports on the silylation of layered silicate, Osterloh et al. firstly reported modification of non-silicate layered material, $HCa_2Nb_3O_{10,}$ with 3-aminopropyltrimethoxysilanes.[43],[44] After that, silylations were reported for various layered crystal such as LDH,[45] layered titanate,[46-49] layered hexaniobate,[50],[51] graphene oxide. [52] ,[53]The reported examples on the silylation of layered crystals are summarized in Table 1. Modifide nanosheets was synthesized by exfoliation of silylated layered crystal with ultrasonication. However, modified nanosheet was not reported that fully exfoliation and stable dispersion of nanosheet colloid.

Table 1 The reported examples on the silylation of layered crystals

Host	Organic molcule	Starting from	Final product	Special notes (Method, etc.)	Reference
Magadiite	trimethylchlorosilane or hexamethyldisilazane	Layered crystal	Layered crystal		Ruiz-Hitzky, E. et al.,Nature 1980, 287, 29-30.
	hexaethyldisilazane and chloromethyldimethylchlorosilane	Layered crystal	Layered crystal		Ruiz-Hitzky, E. et al.,Colloid&PolymerSci, 1985, 263,1025-1030 .
	diphenylmethylchlorosilane	Layered crystal	Layered crystal		Yanagawa, T, et al.,Bull. Chem. Soc. Jpn.1988, 61, 3743-3745.
	allyldimethylchlorosilane	Layered crystal	Layered crystal		Yanagisawa, T. et al.,Solid State lon., 1990, 42, 15-19.
	chlorotrimethylsilane	Layered crystal	Layered crystal		Yanagisawa, T. et al.,React. Solids, 1988, 5, 167-175.
	n-alkylchlorosilane (alkyl chain n = 1,2,4,8,18)	Layered crystal	Layered crystal		Okutomo, S. et al.,Appl. Clay Sci., 1999, 15, 253–264 .
	3-(2-aminoethylamino)propyltrimethoxysilan	Layered crystal	Layered crystal		Zhand, Z. et al., Chem. Mater. 2003, 15, 2921-2925.
	octyltrichlorosilane	Layered crystal	Layered crystal		Fujita, I. et al., Chem. Mater. 2005, 17, 3717-3722.
	3- mercaptopropyl)trimethoxysilane	Layered crystal	Layered crystal		Ide. Y. et al.,Bull. Chem. Soc. Jpn. 2007, 80, 1624–1629.
	2-(perfluorohexyl)-ethyl]trichlorosilane	Layered crystal	Layered crystal		Matsuo, Y. et al., J.Fluor. Chem., 2008, 129, 1150–1155.
	2-(4-chlorosulfonylphenyl) ethyltrimethoxysilane	Layered crystal	Layered crystal		Ide. Y. et al.,Appl. Mater. Interfaces 2012, 4, 2186–2191.
	bis-(triethoxysilylpropyl) polysulfide or 3-mercaptopropyltriethoxysilane	Layered crystal	Layered crystal		Li, S. et al., Colloids Surf. A Physicochem. Eng. Asp., 2016, 506, 320–330.
Kenyaite	diphenylmethylchlorosilane	Layered crystal	Layered crystal		Yanagisawa, T, et al.,Bull. Chem. Soc. Jpn.1988, 61, 3743-3745.
	chlorotrimethylsilane	Layered crystal	Layered crystal		Yanagisawa, T. et al.,React. Solids, 1988, 5, 167-175.
Kanemite	trichloro(alkyl)silanes (alkyl chain n = 1,2,4,8,18)	Layered crystal	Layered crystal		Shimojima, A., et al., Chem. Mater. 2001, 13, 3603-3609
Octosilicate	dialkoxydichlorosilane ((CnO)2Si-Oct, n) 4, 6, 8, 10, and 12)	Layered crystal	Layered crystal		Mochizuki. D. et al.,J. Am. Chem. Soc. 2002, 124, 12082-12083.
	n-Alkoxytrichlorosilane (n = 6, 8, 10, and 12)	Layered crystal	Layered crystal		Mochizuki. D. et al.,J. Am. Chem. Soc. 2005, 127, 7183-7191.

Octosilicate	octyltrichlorosilane	Layered crystal	Layered crystal		Fujita, I. et al., Chem. Mater. 2005, 17, 3717-3722.
	1,4-bis(trichloro- and dichloromethyl-silyl)benzenes	Layered crystal	Layered crystal		Mochizuki, D. et al., Chem. Mater. 2006, 18, 5223-5229.
	3-mercaptopropyl)trimethoxysilane.	Layered crystal	Layered crystal		Ide. Y. et al.,Langmuir 2009, 25(9), 5276–5281.
	(1-butyl)- 3-(3-triethoxysilylpropyl)-4,5-dihydroimidazolium chloride or (1-octyl)- 3-(3-triethoxysilylpropyl)-4,5-dihydroimidazolium chloride	Layered crystal	Layered crystal		Takahashu, N. et al., Chem. Mater. 2010, 22, 3340–3348.
	octadecyltrichlorosilane and phenyltrichlorosilane	Layered crystal	Layered crystal		Ide. Y. et al., Langmuir 2011, 27, 2522–2527.
	(1-butyl-3-(3-triethoxysilylpropyl)-4,5-dihydroimidazolium chloride)	Layered crystal	Nanosheet		Takahashi, N. et al., Chem. Mater. 2011, 23, 266–273 .
	phenethyl(dichloro)methylsilane.	Layered crystal	Layered crystal		Nakamura, T. et al., Langmuir 2012, 28, 7505−7511.
RUB – 51	dichlorodimethylsilane and trichloromethylsilane	Nanosheet	Nanosheet		Asakura, Y. et al., Bull. Chem. Soc. Jpn., 2011, 84, 968-975.
Kaolinite	2-(3-(diethylamino)-6-(diethylimino)-6H- xanthen-9-yl)-N-(3-	Layered crystal	Layered crystal		Sas, S. et al.,Appl. Clay Sci. 2015, 108, 208–214.
Saponite	3-aminopropyltriethoxysilane	Layered crystal	Layered crystal		Qi, T. et al., Appl. Clay Sci., 2016, 132–133, 133–139.
Montmorillonite	n-alkyltrialkoxysilane (alkyl chain n = 1,3,4,6,8,12,18)	Nanohseet (dried)	Nanohseet (dried)		Onikata. M. et al.,Clay Sci., 1995, 9, 299-310.
	3-aminopropyltriethoxysilane	Layered crystal	Layered crystal		Park, K. W. et al.,Bull. Korean Chem. Soc. 2004, 25, 965-968.
	bis-bromo-triethoxysilane	aggregateed nanosheets	aggregateed nanosheets	Follwed by polymeriaztion of PNIPAAm	Chen, Y-M. et al., Chem. Mater. 2009, 21, 4071–4079.
	3-aminopropyltriethoxysilane, N-(2-aminoethyl)-3-	Layered crystal	Layered crystal		Piscitelli, F. et al., J. Colloid and Interface Sci., 2010, 351,108–115.
	rhodamine B derivative carrying an alkoxysilane moiety and neutral	Layered crystal	Layered crystal		Bujdák, J. et al., Appl. Clay Sci., 2012, 65–66, 152–157.
	3-mercaptopropyl)triethoxysilane	Layered crystal	Layered crystal		Bertuoli. P. T. et al.,Appl. Clay Sci.,2014, 87,46–51.
	dimethylchlorovinylsilane and trichlorovinylsilane	Layered crystal	Layered crystal		Sepehri. S. et al.,Appl. Clay Sci.,2014, 97-98, 235–240.
	bis-bromo-triethoxysilane	Layered crystal	Layered crystal	Follwed by polymeriaztion of PNIPAAm	Lie, H-C. et al., Colloids Surf. B, 2017, 152, 459–466.

$KTiNbO_5$	polysiloxane	colloidal nanoplatelet	aggrigation of nanoplatelet	Bruzaud. S. et al.,Chem. Mater. 2002, 14, 2421-2426
$Ca_2Nb_3O_{10}$	3-aminopropyltrimethoxysilane	Nanosheet	Nanosheet	Osterloh. F. E., et al., J. Am. Chem. Soc. 2002, 124, 6248-6249
	3-aminopropyltriethoxysilane	Nanosheet	aggrigation of nanosheets	Kim. J. Y. et al.,J. Phys. Chem. B 2005, 109, 11151-11157
	poly(dimethylsiloxane) and tetramethoxysilane	Nanosheet	Nanosheet	Tahara. S. et al.,Chem. Mater. 2005, 17, 6198-6204.
$K_{0.8}Ti_{1.73}La_{0.27}O_4$	n-octadecyltrimethoxysilane	Layered crystal	Layered crystal	Ide. Y. et al.,Chem. Lett., 2005, 34, 1240-1241.
	phenyltrime thoxysilane	Layered crystal	Layered crystal	Ide. Y. et al.,Angew. Chem. Int. Ed. 2007, 46, 8449 –8451.
$K_2Ti_4O_9 \cdot nH_2O$	n-alkyltrimethoxysilane (alkyl chain n = 1,3,4,6,8,12,18)	Layered crystal	nanohseet	Ide. Y. et al.,J. Colloid Interface Sci.,2006,296,141-149.
$K_4Nb_6O_{17} \cdot 3H_2O$	octadecyltrimethoxysilane	Layered crystal	Layered crystal	Nakato, T. et al.,Chem.-Lett. 2007, 136,1240-1241.
Layered tungstates ($H_2W_2O_7$)	3-mercaptopropyltrimethoxysilane	Nanosheet	Nanosheet	Mochizuki, D. et al.,Angew. Chem. Int. Ed. 2012, 51, 5452 –5455
$HxTi_{(2-x)/4}\square_{x/4}O_4$	allyltrimethoxysilane	Nanosheet	Nanosheet	
Layered double hydroxide	3-aminopropyltriethoxysilane	Layered crystal	Layered crystal	Park, A-Y. *et al.,* Advanced Materials, 2005, 17, 106-109.
	3-aminopropyltriethoxysilane	Layered crystal	Layered crystal	Tao, Q. et al.,Applied Surface Science, 2009, 255, 4334–4340.
	trimethylchlorosilane, tetraethoxysilane and dimethyldiethoxylsilane	Layered crystal	Layered crystal	Tao, Q. et al., J.Solid State Chem., 2014, 213, 176–181.
	phenyltriethoxysilane	Layered crystal	Layered crystal	Gue, W. et al., Applied Catalysis A: General, 2016, 522, 101–108
	triethoxyvinylsilane, triethoxyoctylsilane and (3-gylcidyloxypropyl)trimethoxysilane	Layered crystal	Layered crystal	Chen, C. et al., Dalton Trans., 2020, 49, 8498–8503.
$Cs_{0.67}Ti_{1.83}O_4$	3-aminopropyltriethoxysilane	Layered crystal	Layered crystal	Kim. T. W. et al.,Sci. Rep. 2016, 6, 1-12.
Graphite oxide	(*N*-(trimethoxysilyl- propyl) ethylenediamine triacetic acid sodium	nanohseet	nanohseet	Hou, S. et al., J. Phys. Chem. C 2010, 114, 14915–14921.
	3- aminopropyltriethoxysilane	nanohseet	nanohseet	Wang, X. et al., Compos. Sci. Technol., 2012, 72, 737–743.
	hexadecyltrimethoxysilane	nanohseet	nanohseet	Ma, W.-S. et al., J. Mater. Sci., 2013, 48, 156–161.
	trimethoxy(7-octen-1-yl)silane with polydimethylsiloxane and	nanohseet	nanohseet	Guimont, A. et al., Polymer, 2013, 54, 4830-4837.

Graphite oxide	3-aminopropyl- triethoxysilane	Nanohseet	Nanohseet		Ma, W. et al., Colloid. Polym. Sci., 2013, 291/2765–2773.
	allyltrimethoxysilane	Nanohseet	Aggregateed of nanosheets		Pazat, A. et al., Appl. Surf. Sci., 2017, 396, 902–911.
	1-(trimethox- ysilyl)propyl-3-methylimidazolium	Nanohseet	Nanohseet		Zhu, J. et al., Catal. Lett.,2017, 147, 335–344.
	of N-(2-aminoethyl)-3-(trimethoxysilyl)propylamine	Nanohseet	Nanohseet	Followed by glutaraldehyde and ssDNA having end of FAM and	Kahyaoglu, L. N. et al.,Langmuir 2018, 34, 14586−14596.
	polyaminopropylmethylsiloxane-b-polydimethylsiloxane copolymer	Nanohseet	Nanohseet		Zhang, Z. et al., Compos. B, 2019, 176, 107338.
	3-(trimethoxysilyl)propylmethacrylate	Nanohseet	Nanohseet		Shah, S. et al., Pak. J. Anal. Environ. Chem., 2020, 21, 44-53.
α-Zirconium phosphate	octadecyltrichlorosilane	Nanoplatelet	Nanoplatelet		Díaz. A. et al.,Chem. Mater. 2013, 25, 723−728
	monomethoxy−polyethyleneglycol−monophosphate	Layered crystal	Layered crystal		Bakhmutov. V. I. et al., Magn. Reson. Chem. 2017, 55, 648–654.
Mxene	3-aminopropyltriethoxysilane, hexadecyltrimethoxysilane and 1H,1H, 2H,2H-Perfluorodecyltriethoxysilane	Nanosheet	Nanosheet		Ji, J. et al., FlatChem 2019, 17, 100128.

1.3.2 Alcohols

This chapter describes modification of alcohols onto the layered crystal. Organic derivative is generated to modify of alkoxyl group onto interlayer surface of layered crystal though a covalent bond by condensation reaction of hydroxyl group of alcohol with hydroxyl group of layered crystal surface. While the reported of silylation of layered crystal, Takahashi et al. firstly reported modification of methanol onto interlayer of layered perovskite($HLaNb_2O_7$). [54] However, Si-O-C bond of generated derivative by this reaction is known to be vulnerable to alcoholysis and hydrolysis than Si-O-Si bond of generated derivative by silylation. Also, Suzuki et al. reported that the modified alkoxyl group on the layered perovskite was substituted with other alkoxyl groups by reaction in the specific alcohols.[55] (Figure1-8) Boykin et al. reported modification of *n*-alcohols onto layered perovskite by new modification method using the microwave. [56] The reported examples on the modification of layered crystals with alcohols are summarized by Wang et al. in Table 2.[57]

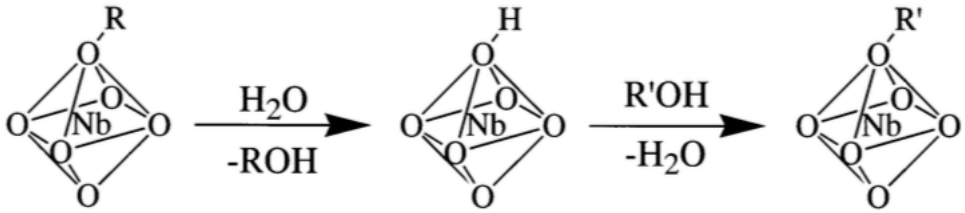

FIgure 1-8 Schematic representation of proposed reaction mechanism[55]

Table 2 typical grafting reactions of alcohols onto layered crystal[57]

Phase	Protonated form	Intermediate	Organic phase	Solvent	Method	T	t
Dion–Jacobson	$HLaNb_2O_7$ (HLN)	∅	Methanol	Water added	Stirring	R.T.	1 d
		∅	Ethanol	Water added	Stirring	R.T.	7 d
		∅	*n*-Alcohol, $n_C = 3$–6, 8, 10, 12	Water added	Classical heating	80 °C	7 d
		n-Decoxyl-HLN	2-Propanol, ethylene glycol	Water added	Solvothermal	80 °C	7 d
		n-Decoxyl-HLN	*tert*-Butyl alcohol	Water added	Solvothermal	80 °C	14 d
		n-Decoxyl-HLN	*n*-$C_nH_{2n+1}PO(OH)_2$, $4 \leq n \leq 18$	2-Butanone + 1% water	Classical heating	80 °C	2–3 d
		n-Decoxyl-HLN	*n*-$CH_3(OCH_2CH_2)_nOH$, $1 \leq n \leq 4$	∅	Classical heating	80 °C	14 d
		n-Decoxyl-HLN	$CF_3(CF_2)_7C_2H_4OH$	2-Butanone + 1% water	Classical heating	80 °C	7 d
		n-Decoxyl-HLN	D-Glucopyranose	2-Butanone + 10% water	Solvothermal	70 °C	3 d
		Propoxyl-HLN	CF_3COOH	∅	Solvothermal	70 °C	3 d
		Propoxyl-HLN	4-Penten-1-ol	∅	Solvothermal	80 °C	7 d
		∅	Methanol or propanol	Water added	Microwave	100 °C	1 h
		Methoxyl-HCN	*n*-Propanol	Water added	Microwave	100 °C	1 h
		Methoxyl-HCN or propoxyl-HCN	*n*-Pentanol	Water added	Microwave	120 °C	1 h
		Methoxyl-HCN or propoxyl-HCN	*n*-Decanol	Water added	Microwave	150 °C	0.5 h
	$HCa_2Nb_3O_{10}$ (HCaN)	∅	Methanol or ethanol	Water added	Solvothermal	150 °C	7 d
		Methoxyl-HCaN	*n*-Propanol	Water added	Solvothermal	150 °C	7 d
		Propoxyl-HCaN	*n*-Alcohol, $4 \leq n_C \leq 18$	Water added	Solvothermal	150 °C	7 d
	$HSr_2Nb_3O_{10}$ (HSN)	∅	Methanol	Water added	Microwave	Not-mentioned	4 h
		Methoxyl-HSN	*n*-Propanol	Water added	Microwave	Not-mentioned	4 h
		Propoxyl-HSN	*n*-Hexanol	Water added	Microwave	Not-mentioned	3.5 h
Ruddlesden–Popper	$H_2CaTa_2O_7$ (HCT)	Methylamine-HCT	Methanol	Water added	Solvothermal	100 °C	3 d
		Methoxyl-HCT	*n*-Propanol	Water added	Solvothermal	80 °C	7 d
		Propoxyl-HCT	*n*-Alcohol, $n_C = 6$, 10	Water added	Solvothermal	80 °C	7 d
		n-Decoxyl-HCT	D-Glucopyranose	2-Butanone + 10% water	Solvothermal	70 °C	3 d
		Propylamine-HCT	*n*-Propanol	Water added	Microwave	110 °C	1 h
		Propoxyl-HCT	*n*-Alcohol, $n_C = 5$, 10	∅	Microwave	120 °C	1 h
	$H_2La_2Ti_3O_{10}$ (HLT)	*n*-Butylamine-HLT	*n*-Propanol	Water added	Solvothermal	180 °C	5 d
		Propoxyl-HLT	*n*-Alcohol, $n_C = 4$, 8, 10, 12	Water added	Solvothermal	150 °C	5 d
Aurivillius	$H_2Bi_{0.1}Sr_{0.85}Ta_2O_7$ (HST)	Ethylamine-HST	Ethanol	Water added	Microwave	130 °C	2 h
		Ethoxyl-HST	4-Pentyn-1-ol	Water added	Microwave	110 °C	2 h

1.3.3 Phosphoric acid derivative

This chapter describes modification of phosphoric acid derivatives onto layered crystal. The chemically stable M-O-P bond (M is Nb, Al, etc.) is generated by reaction of hydroxy group of layered crystal surface with phosphoric acid group of a phosphoric acid derivative. Phosphoric acid derivatives have less tendency to homo-condense than silane coupling agents due to high stably. Sugahara et al. reported modification of phosphoric acid derivative onto the interlayer of layered HLaNb using intermediate as n-decoxy derivatives of HLaNb.[58](Figure 1-9)

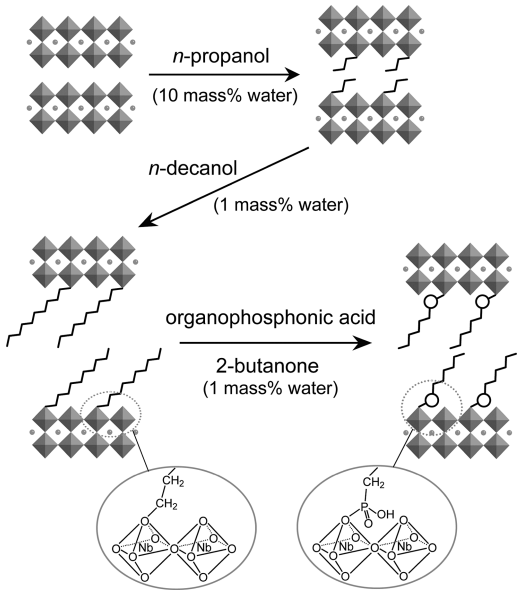

FIgure 1-9 Overviw of the modification of the ion-exchange-able layered perovskite HLaNb with organicphosphonic acids[58]

Kimura et al. reported synthesis of single and double layered organically modified nanosheet by change of kinds of the alkylammonium ions which is intercalated into layered hexaniobate having two types of interlayer.[59] Sugahara et al. reported that janus nanosheet was synthesized by modification of octadecylphosphoric acid onto interlayer I of dimethyldioctadecylammonium ion intercalated layered hexaniobate, followed by modification of carboxypropylphosphoric acid onto the interlayer II.[60] Machida et al reported that Kaolinite was modified with triethylphosphhine oxide.[61]
While the layered crystals have been used for grafting reactions, exfoliated single layer nanosheets were directly modified recently. Sugahara et al. reported modification of the exfoliated HLaNb nanosheets with octadecylphosphoric acid by biphasic system

reaction.[62] (Figure 1-10) Chen et al. have reported modification of the exfoliated MXene nanosheet with octadecylphosphoric acid by biphase system reaction at the same time. [63]Also, Sugahara et al. have reported new modification method by biphase system reaction using a micro fluidics device; reaction of HLaNb nanosheet with octadecylphosphoric acid proceeded at higher modification rate than previous report in shorter reaction time.[64] The reported examples on the modification of phosphoric acid derivatives onto layered crystals are summarized in Table 3.

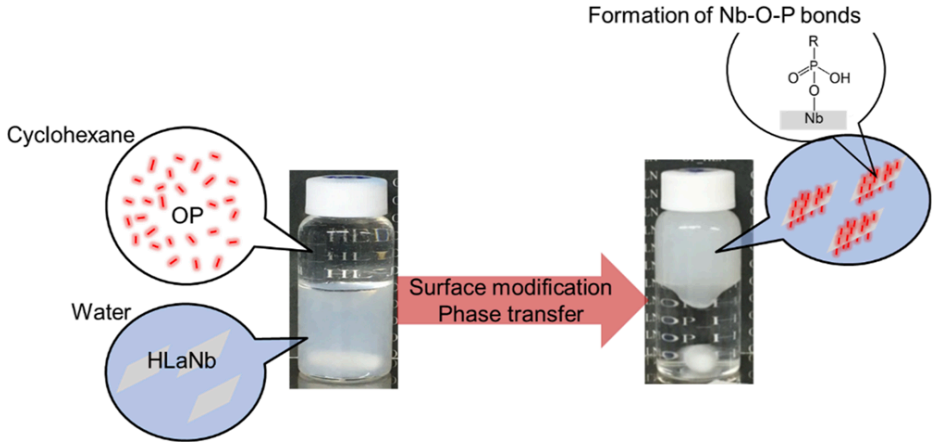

Figure 1-10 Modification of octadecylphosphoric acid onto HLaNb nanosheet by biphase system[62]

Table 3 The reported examples on the modification of phosphoric acid derivative of layered crystals

Host	Organic molcule	Starting from	Final product	Special notes (Method, etc.)	Reference
$HLaNb_2O_7 \cdot xH_2O$	n-alkylphosphonic acid, (alkyl chain= 4, 6, 8, 10, 12, 18)	Layered crystal	Layered crystal		Shimada, A. et al., Chem. Mater. 2009, 21, 4155–4162
	m-(chloromethyl)phen- ylmethylate	Layered crystal	Layered crystal	Follwed by polymeriaztion of	Idota, N. et al., Chem. Lett. 2015, 44, 203–205.
	triethylphosphhine oxide	Layered crystal	Layered crystal		Toihara, N. et al., Dalton Trans., 2015, 44, 3002–3008.
	oleyl phosphate	Nanosheet	Nanosheet	Biphasic system	Sugaya et al., Langmuir 2019, 35, 6594–6601.
	oleyl phosphate	Nanosheet	Nanosheet	Biphasic system, using microfluidic device	Sugaya, T. et al., Langmuir 2020, 36, 7252–7258.
Layered double hydroxide	KH_2PO_4	Layered crystal	Layered crystal		Shimamura, A. et al., J. Solid State Chem. 2012, 186, 116–123
$KCa_2Nb_3O_{10}$	phenylphosphonate	Layered crystal	Layered crystal		Shori, S. et al., J. Colloid Interf. Sci. 2015, 437, 97-110
$K_4Nb_6O_{17} \cdot 3H_2O$	octadecylphosphonic acid and carboxypropylphosphonic acid	Layered crystal	Nanosheet	Janus nanoshet	Suzuki, R. et al., Chem. Commun., 2018, 54, 5756-5759.
	phenylphosphonic acid	Layered crystal	Nanosheet		Kimura, N. et al., Langmuir 2014, 30, 1169–1175.
α-Zirconium phosphate	monomethoxypolyethyleneglycol monophosphate	Layered crystal	Layered crystal		Bakhmutov. V. I. et al., Magn. Reson. Chem. 2017, 55, 648–654.
Kaolinite	triethylphosphate	Layered crystal	Layered crystal		Machida, S. et al., Langmuir 2018, 34, 12694–12701.
	trimethylphosphate	Layered crystal	Layered crystal		Machida, S. et al., Dalton Trans., 2019, 48, 11663.
$Ti_3C_2T_x$(MXene)	n-alkylphosphonic acid (alkyl chain=8, 10, 12)	Nanosheet	Nanosheet	Biphasic system	Kim. D., et al., ACS Nano 2019, 13, 13818–13828.

1.3.4 Other modification species

In this section, the modification of layered crystal with other organic species will be reviewed. Layered crystal surface such as graphene oxide and α-zirconium phosphate is able to modify organic molecule with amino group and isocyanate group due to the interlayer surface of layered crystal with highly reactive functional group such as carboxyl group and phosphate group.

Stankovich et al. reported modification of 4-tscocyanatobenzenesulfonyl azide onto graphene oxide platelet surface followed by dispersion of the sample in the DMF.[65] Graphene and graphene oxide were modified with various types of organic molecules such as ATRP initiator, ionic liquid, 1-(3-aminopropyl)imidazole, phenyl isocyanate. Ohno et al. reported synthesis of PMMA grafted graphene oxide which form liquid crystal phase in a mixture of o-dichlorobenzene/1,2-dichloroethane by modification of ATRP initiator onto the surface followed by ATRP polymerization of MMA. [66] (Figure 1-11)

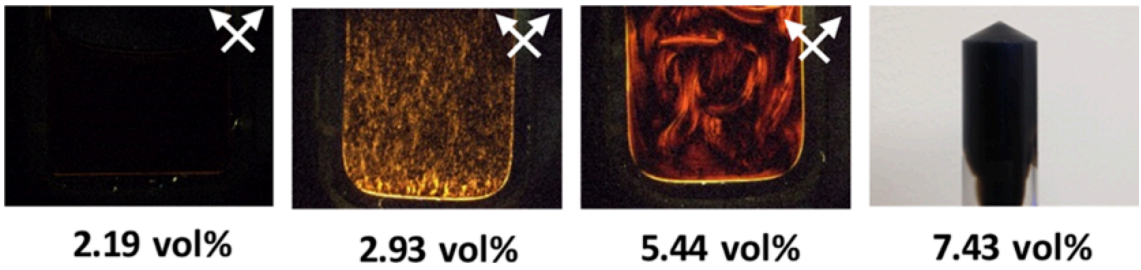

Figure 1-11 Digital microscopy images of suspensions of GO end-grafted with PMMA brushes in a 68/32 (v/v) mixture of *o*-dichlorobenzene/1,2-dichloroethane, as observed using two crossed polarizers.[66]

Mejia et al. reported modification of octadeyl isocyanate onto α-zirconium phosphate.[67] Also, Baker et al. reported dispersion of modified nanoplatelets into organic solvent such as THF and DMF by modification of M1000 or alkyl Glycidyl Ethers onto α-zirconium phosphate. Studies of modification onto layered crystal and nanosheet were reported silane coupling agents, alcohols, polymer having end of functional group and so on. [68]However, Sato et al. firstly reported modification of cellulose which is functional molecule like biomolecule onto $HLaNb_2O_5$.[65] The reported examples on the modification of organic molecules having isocyanate group, amino group and ATRP initiator onto layered crystals are summarized in Table 4.

Table 4 The reported examples on the modification of other modification species of layered crystals

Host	Organic molcule	Starting from	Final product	Special notes (Method, etc.)	Reference
α−Zirconium Phosphate	octadecyl isocyanate	Layered crystal	Few stacked nanosheet		Mejia, F. A. et al., Soft Matter, 2012, 8, 10245-10253.
	M-1000,glycidyl methacrylate and cyclohexene oxide	Nanoplatelet	Nanoplatelet		Baker, J. et al., Langmuir 2020, 36, 11948−11956.
Graphen Oxide	4-isocyanatobenzenesulfonyl azide	Layered crystal	Layered crystal		Stankovich, S.et al. Carbon 44 (2006) 3342–3347.
	sodium dodecylbenze- nesulfonate	Few stacked nanosheet	Few stacked nanosheet		Lomeda, J. R., et al., J. Am. Chem. Soc. 2008, 130, 16201–16206.
	4- nitrophenyl diazonium	Nanosheet	Nanosheet		Bekyarova, E., et al., J. Am. Chem. Soc. 2009, 131, 1336–1337.
	4-bromoaniline	Nanosheet	Nanosheet		Sun, Z., Nano Res, 2010, 3, 117–125
	2-bromo-2- methylpropionyl bromide	Nanosheet	Nanosheet	Followed by polymerization of styrene	Goncalves, G. et al. J. Mater. Chem., 2010, 20, 9927–9934.
	4-aminophenol	Nanohseet	Nanohseet	Followed by Triethylamine and polymerization of NIPAM	Ren, L. et al., J. Nanopart. Res., 2012, 14, 940.
	1-(3-aminopropyl)imidazole	Nanosheet	Nanosheet		Liu, W. et al., J. Mater. Chem., 2012, 22, 18395–18402.
	2-bromoisobutyryl bromide	Nanosheet	Nanosheet	Followed by polymerization of MMA	Leon, A. C. et al., ACS Nano 2017, 11, 7485−7493.
	1-amino-2-((3-((2-bromo-2-methylpropanoyl)oxy)propyl)thio)-	Nanosheet	Nanosheet	Followed by polymerization of MMA, modified nanosheets	Ohno, K. et al. Langmuir 2019, 35, 10900−10909.
Magadiite	ethylene sulfide	Layered crystal	Layered crystal		Oliveira, M.M., et al., Microporous Mesoporous Mater., 2014, 196, 292–299.
$HLaNb_2O_7 \cdot xH_2O$	cellulose	Nanosheet	Nanosheet		Sato, S. et al., Cellulose, 2017, 24, 5463–5473.

1.4 Composite of DNA and nanosheet

1.4.1 DNA

DNA is an abbreviation for deoxyribonucleic acid, which is a biopolymer that carries the genetic information of living organisms. Biologically, it is a substance that remembers programs essential for vital functions such as morphogenesis and metabolic systems of living organisms. In 1953, Watson, Crick et al. reported that DNA has a structure in which two string-like molecules are spirally entwined, that is called a double helix structure. The diameter of the helix is about 2 nm, and one rotation (pitch) of the helix is about 3.4 nm with 10.5 base pairs.[69]

There are two type pf grooves of different widths in the double helix of DNA. A wide groove is called a major groove, and a narrow groove is called a minor groove. The state in which two string-like molecules are entangled to form a double helix structure is called double-stranded DNA (dsDNA), and the state in which each DNA is separated is called single-stranded DNA (ssDNA). The persistent length of dsDNA is known to be 50 nm (about 150 base pairs), and below the length, it can be regarded as a hard rod-like molecule. On the other hand, ssDNA has 0.7 nm (about 2 bases) and a diameter of about 1 nm, indicating that it is a very flexible polymer. DNA is a polymer in which units called nucleotides are connected, and these nucleotides are composed of phosphoric acid, bases, and sugars. A compound in which a base is bonded to the carbon at the 1'position of a sugar is called a nucleoside, and a compound in which phosphoric acid is ester-bonded to the 5'position of the nucleoside is called a nucleoside. The carbon atoms at the 3'and 5'positions of this nucleotide are linked via phosphoric acid to form a chain molecule, and this phosphate-sugar-phosphoric acid site is called the backbone. There are four types of DNA bases as shown Figure1-12: Adenine, Guanine, Cytosine, and Thymine.

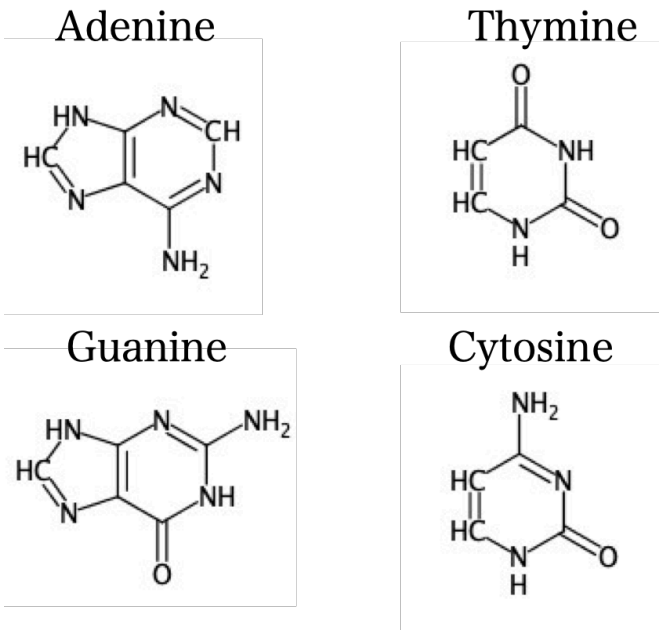

Figure 1-12 Types of DNA bases

A DNA base sequence in which these bases are repeatedly linked is called a DNA base sequence. The bases of DNA are bound by hydrogen bonds, but form base pairs only between adenine and thymine, and guanine and cytosine. This is called base complementarity, and a stable double helix cannot be formed unless the base sequences of each other are complementary. When heat is applied to the DNA forming the double helix in the solution, the double-stranded DNA separates into single strands. This reaction is called denaturation or melting, and conversely, the formation of double strands by two single-strand DNAs is called hybridization. DNA is a stable substance from 0 ° C to about 100 ° C, and hybridization and denaturation can be repeated many times by repeating cooling and heating. Since there are two hydrogen bonds between adenine and thymine and three hydrogen bonds between guanine and cytosine, it can be seen that the bond between guanine and cytosine is stronger than that between adenine and thymine. Therefore, in general, the higher the content of guanine and cytosine, the greater the stability of the structure. Being able to quantitatively handle the strength of the double helix bond of DNA in this way is important in the construction of DNA information processing devices and the structure of DNA.

1.4.2 DNA nanotechnology

DNA nanotechnology is a technology for designing nanostructures by changing the base sequence of DNA. In DNA nanotechnology, it is possible to form free and large-scale nanostructures by designing the base sequence of DNA. This DNA nanotechnology originated from the idea that Seeman formed a structure by combining the double helix structures formed by DNA in the 1980. However, at that time, a complicated reaction procedure using an enzyme was required, and the yield was low. However, in around 2000, [70] a new methodology was devised for structural design of DNA by associating the self-assembly process of DNA with parallel computing of computers. This made it possible to form a flat structure like a tile. On the other hand, in 2006, a method called DNA origami was reported in Rothemund in which long DNA was folded like a protein to form a planar structure.[71](Figure 1-13) DNA origami is designed using design software, etc., and a structure of about 100 nm can be synthesized by self-assembly of DNAs. A circular long-chain ssDNA called scaffold DNA (generally using a phage called M13mp18 of about 7,000 bases) and a chemically synthesized short ssDNA called staple DNA (several tens of bases) are mixed, heated, and slowly. By cooling, a large amount of nanostructures as designed can be synthesized. Although the DNA structure itself does not have a special function, it can be used as a reaction field by immobilizing a molecule or the like on the structure. In addition, by combining two-dimensional structures, a three-dimensional structure can be formed, which can be expected to be used as capsules and containers such as DDS. Furthermore, it is possible to develop a molecular robot by creating a three-dimensional structure using DNA origami as a skeleton and incorporating other functional molecules and molecular devices. By combining DNA with other substances in this way, further development of DNA nanotechnology can be expected.

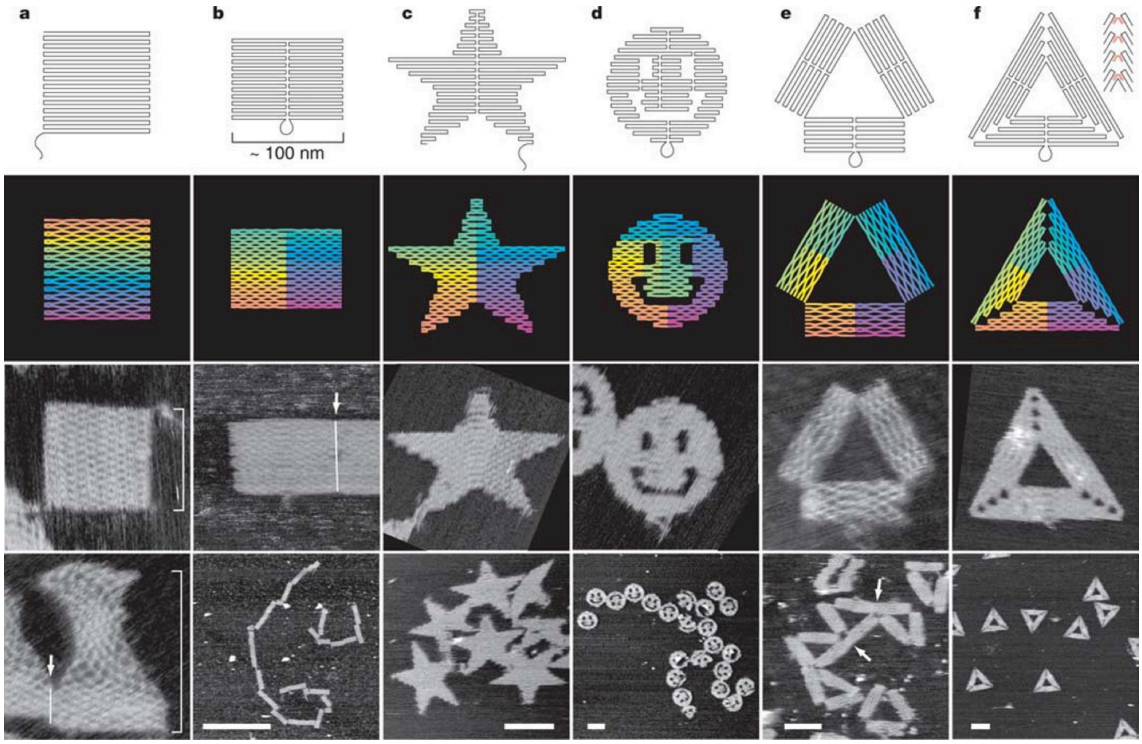

Figure 1-13 DNA origami shapes. Top row, folding paths. a, square; b, rectangle; c, star; d, disk with three holes; e, triangle with rectangular domains; f, sharp triangle with trapezoidal domains and bridges between them [71]

1.4.3 Composite of DNA and nanomaterials

There have been many reports of attempts to control the spatial arrangement of colloidal particles by using DNA as a linker. The most frequently reported are gold nanoparticles. By modifying the surface of gold nanoparticles with DNA and mixing gold nanoparticles with different linker DNAs, colloidal crystals are formed[72] and lattice constants are controlled[73] and so on. Construction or control of the structure of colloidal particles using such DNA shows the usefulness of the DNA functionalization system, and can impart new functions to colloidal crystals such as biosensing and synthesis of metamaterials.

1.4.4 Composite of DNA and nanosheet

Several cases of complexation of DNA and nanosheets have been reported. A biosensor that mainly adsorbs ssDNA having a fluorescent molecule at the end on the surface of the nanosheet and hybridizes it so that it peels off from the nanosheet and exhibits fluorescence. [74],[75],[76] In addition, when graphene and dsDNA are mixed and heated,

dsDNA becomes ssDNA, and ssDNA crosslinks between graphene to gel, which is a stimulus-responsive gel. [77] The surface of titanium oxide nanosheets is modified with aminoalkylsilane to form dsDNA. Nanocontainers have been reported that add and form aggregates by interaction with the main hall and release internal substances when heated . [78] Furthermore, the most similar to this study is the successful formation of aggregates by adsorbing ssDNA to graphene and adding ssDNA having a complementary base sequence8. (Figure 1-14) [79]

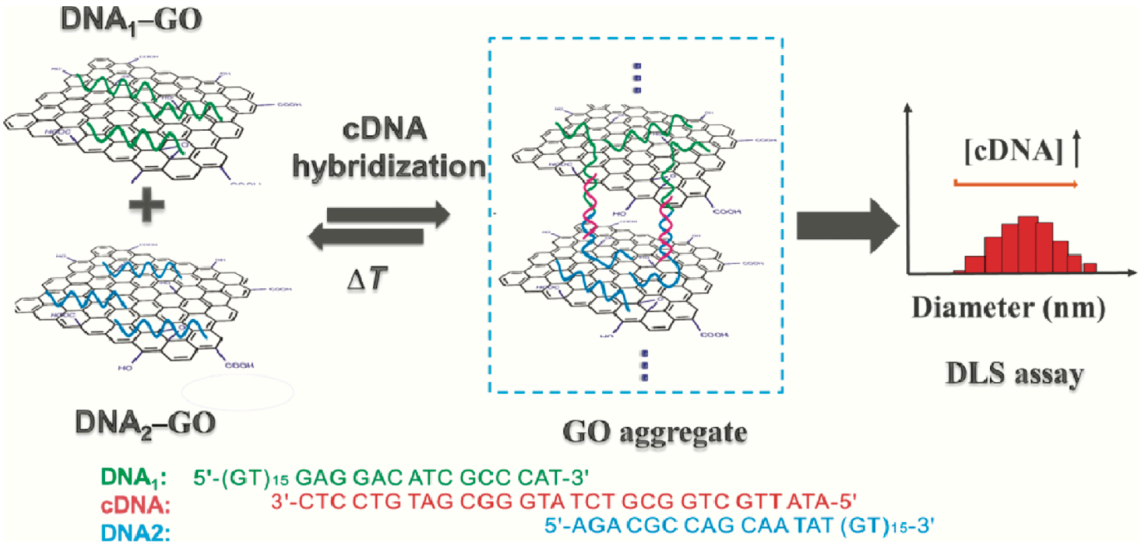

Figure 1-14 Schematic illustration of procedures for DNA-directed self-assembly of graphene oxide and homogeneous detection of DNA by dynamic light scattering technique.[79]

1.5 Reference

1. G.Lagaly, Characterrization of Clay by Organic Compounds. *Clay Miner.* **1981,** *16*, 1-26.

2. Brindley, G.W.; Semples, R. E., Preparation and properties of some hydroxy-alminium beidellites. *Clay Miner.* **1977**, 12, 229-237

3. Kojima, Y.; Usuki, A.; Kawasumi, M.; Okada, A.; Fukushima, Y.; Kurauchi, T.; Kamigaito, O., Mechanical properties of nylon 6-clay hybrid. *J. Mater. Res.* **1993,** *8* (5), 1185-1189.

4. Domen, K.; Kudo, A.; Shibata, M.; Tanaka, A.; Maruya, K.-I.; Onishi, T., Novel photocatalysts, ion-exchanged K4Nb6O17, with a layer structure. *Chem. Comm.* **1986,** *23*, 1706-1707.

5. Tsuneo Yanagisawa; Masatoshi Harayama; Kuroda, K.; Kato, C., Organic Derivatives of Layered Polysilicates I. Trimethylsilylation of Magadiite and Kanyaite. *Reactivity of Solids* **1988,** *5*, 167-175.

6. F.Livolant; A.M.Levelut; J.Doucet; J.P.Benoit, The highly concentrated liquid-crystalline phase of DNA is columnar hexagonal. *NATURE* **1989,** *339*, 724-726.

7. D.Frenkel; H.N.W.Lekkerkerker; A.Stroobants, Thermodynamic stability of a smectic phase in a system of hard rods. *NATURE* **1988,** *332*, 822-823.

8. van der Kooij, F. M.; Lekkerkerker, H. N. W., Formation of Nematic Liquid Crystals in Suspensions of Hard Colloidal Platelets. *J. Phys. Chem. B* **1998,** *102*, 7829-7832.

9. Gabriel, J. C. P.; Camerel, F.; Lemaire, B. J.; Desvaux, H.; Davidson, P.; Michael, W.; Batail, P., Swollen liquid-crystalline lamellar phase based on extended solid-like sheet. *Nature* **2001,** *413*, 504-508.

10. Sun, D.; Sue, H.-J.; Cheng, Z.; Martínez-Ratón, Y.; Velasco, E., Stable smectic phase in suspensions of polydisperse colloidal platelets with identical thickness. *Physical Review E* **2009,** *80* (4), No. 041704.

11. Miyamoto, N.; Nakato, T., Liquid crystalline nature of $K_4Nb_6O_{17}$ nanosheet sols and their macroscopic alignment. *Adv. Mater.* **2002,** *14* (18), 1267-1270.

12. Nakato, T.; Miyamoto, N.; Harada, A., Stable liquid crystalline phases of colloidally dispersed exfoliated layered niobates. *Chem. Comm.* **2004,** (1), 78-79.

13. Nakato, T.; Yamashita, Y.; Kuroda, K., Mesophase of colloidally dispersed nanosheets prepared by exfoliation of layered titanate and niobate. *Thin Solid Filims*

2006, *495* (495), 24-28.

14. Miyamoto, N.; Nakato, T., Liquid crystalline nanosheet colloids with controlled particle size obtained by exfoliating single crystal of layered niobate $K_4Nb_6O_{17}$. *J. Phys. Chem. B* **2004,** *108*, 6152-6159.

15. Miyamoto, N.; Yamamoto, S.; Shimasaki, K.; Harada, K.; Yamauchi, Y., Exfoliated Nanosheets of Layered Perovskite $KCa_2Nb_3O_{10}$ as an Inorganic Liquid Crystal. *Chem. Asian J.* **2011,** *6*, 2936-2939.

16. Langmuir, I., The Role of Attractive and Repulsive Forces in the Formation of Tactoids, Thixotropic Gels, Protein Crystals and Coacervates. *J. Chem. Phys.* **1938,** *6* (12), 873-896.

17. Paineau, E.; Antonova, K.; Baravian, C.; Bihannic, I.; Davidson, P.; Dozov, I.; Impéror-Clerc, M.; Levitz, P.; Madsen, A.; Meneau, F.; Michot, L. J., Liquid-Crystalline Nematic Phase in Aqueous Suspensions of a Disk-Shaped Natural Beidellite Clay. *J. Phys. Chem. B* **2009,** *113*, 15858-15869.

18. Miyamoto, N.; Iijima, H.; Ohkubo, H.; Yamauchi, Y., Liquid crystal phases in the aqueous colloids of size-controlled fluorinated layered clay mineral nanosheets. *Chem. Comm.* **2010,** *46*, 4166-4168.

19. Kim, J. E.; Han, T. H.; Lee, S. H.; Kim, J. Y.; Ahn, C. W.; Yun, J. M.; Kim, S. O., Graphene Oxide Liquid Crystals. *Angew. Chem., Int. Ed.* **2011,** *50* (13), 3043-3047.

20. Aboutalebi, S. H.; Gudarzi, M. M.; Zheng, Q. B.; Kim, J.-K., Spontaneous Formation of Liquid Crystals in Ultralarge Graphene Oxide Dispersions. *Adv. Funct. Mater.* **2011,** *21*, 2978–2988.

21. Miyata, H.; Noma, T.; Watanabe, M.; Kuroda, K., Preparation of Mesoporous Silica Films with Fully Aligned Large Mesochannels Using Nonionic Surfactants. *Chem.Mater.* **2002,** *14* (2), 766-772.

22. Bastakoti, B. P.; Li, Y.; Imura, M.; Miyamoto, N.; Nakato, T.; Sasaki, T.; Yamauchi, Y., Polymeric micelle assembly with inorganic nanosheets for construction of mesoporous architectures with crystallized walls. *Angew. Chem. Int. Ed.* **2015,** *54* (14), 4222-5.

23. Liff, S. M.; Kumar, N.; McKinley, G. H., High-performance elastomeric nanocomposites via solvent-exchange processing. *Nat. Mater.* **2007,** *6* (1), 76-83.

24. E.Ruiz-Hitzky; J.M.Rojo, Intracrystalline grafting on layer silicic acids. *Nature* **1980,** *287*, 28-30.

25. BLANCA CASAL, E. R.-H., Photo-oxidation of Water Mediated by a Clay-anchored Os Catalyst. *Journal of Molecular Catalysis* **1985,** *33*, 83-86.
26. Tsuneo Yanagisawa; Masatoshi Harayama; Kuroda, K.; Kato, C., ORGANIC DERIVATIVES OF LAYERED POLYSILICATES Ill. REACTION OF MAGADIITE AND KENYAITE WITH ALLYLDIMETHYLCHLOROSILANE. *Solid State Ion.* **1990,** *42*, 15-10.
27. Onikata, M.; Kondo, M., Rheological Properties of the Partially Hydrophobic Montmorillonite Treated with Alkyltrialkoxysilane. *Clay Sci.* **1995,** *9*, 299-310.
28. Park, K.-W.; Kwon, O.-Y., Interlamellar Silylation of Montmorillonite with 3-Aminopropyltriethoxysilane. *Bull. Korean Chem. Soc.* **2004,** *25*, No. 7.
29. Fujita, I.; Kuroda, K.; Ogawa, M., Adsorption of Alcohols from Aqueous Solutions into a Layered Silicate Modified with Octyltrichlorosilane. *Chem. Mater.* **2005,** *17*, 3717-3722.
30. Shimojima, A.; Mochizuki, D.; Kuroda, K., Synthesis of silylated derivatives of a layered polysilicate kanemite with mono-, di-, and trichloro(alkyl)silanes. *Chem. Mater.* **2001,** *13* (10), 3603-3609.
31. Mochizuki, D.; Shimojima, A.; Imagawa, T.; Kuroda, K., Molecular Manipulation of Two- and Three-Dimensional Silica Nanostructures by Alkoxysilylation of a Layered Silicate Octosilicate and Subsequent Hydrolysis of Alkoxy Groups. *J. Am. Chem. Soc.* **2005,** *127*, 7183-7191.
32. Mochizuki, D.; Kowata, S.; Kuroda, K., Synthesis of Microporous Inorganic-Organic Hybrids from Layered Octosilicate by Silylation with 1,4-Bis(trichloro- and dichloromethyl-silyl)benzenes. *Chem. Mater.* **2006,** *18*, 5223-5229.
33. Ide, Y.; Fukuoka, A.; Ogawa, M., Preparation of Au Nanoparticles in the Interlayer Space of a Layered Alkali Silicate Modified with Alkylthiol Groups. *Chem. Mater.* **2007,** *19*, 964-966.
34. Asakura, Y.; Matsuo, Y.; Takahashi, N.; Kuroda, K., Ordered Silylation of Layered Silicate RUB-51 with Half-Sodalite Cages. *Bull. Chem. Soc. Jpn.* **2011,** *84* (9), 968-975.
35. Ide, Y.; Iwasaki, S.; Ogawa, M., Molecular recognition of 4-nonylphenol on a layered silicate modified with organic functionalities. *Langmuir* **2011,** *27* (6), 2522-7.
36. Nakamura, T.; Ogawa, M., Attachment of the sulfonic acid group in the interlayer space of a layered alkali silicate, octosilicate. *Langmuir* **2012,** *28* (19), 7505-

11.
37. Chen, Y.-M.; Lin, H.-C.; Hsu, R.-S.; Hsieh, B.-Z.; Su, Y.-A.; Sheng, Y.-J.; Lin, J.-J., Thermoresponsive Dual-Phase Transition and 3D Self-Assembly of Poly(N-Isopropylacrylamide) Tethered to Silicate Platelets. *Chem. Mater.* **2009,** *21* (17), 4071-4079.
38. Piscitelli, F.; Posocco, P.; Toth, R.; Fermeglia, M.; Pricl, S.; Mensitieri, G.; Lavorgna, M., Sodium montmorillonite silylation: unexpected effect of the aminosilane chain length. *J Colloid Interface Sci* **2010,** *351* (1), 108-15.
39. Bujdák, J.; Danko, M.; Chorvát, D.; Czímerová, A.; Sýkora, J.; Lang, K., Selective modification of layered silicate nanoparticle edges with fluorophores. *Applied Clay Sci.* **2012,** *65-66*, 152-157.
40. Bertuoli, P. T.; Piazza, D.; Scienza, L. C.; Zattera, A. J., Preparation and characterization of montmorillonite modified with 3-aminopropyltriethoxysilane. *Applied Clay Sci.* **2014,** *87*, 46-51.
41. Sepehri, S.; Rafizadeh, M.; Hemmati, M.; Bouhendi, H., Study of the modification of montmorillonite with monofunctional and trifunctional vinyl chlorosilane. *Appl. Clay Sci.* **2014,** *97-98*, 235-240.
42. Lin, H. C.; Su, Y. A.; Liu, T. Y.; Sheng, Y. J.; Lin, J. J., Thermo-responsive nanoarrays of silver nanoparticle, silicate nanoplatelet and PNiPAAm for the antimicrobial applications. *Colloids Surf. B* **2017,** *152*, 459-466.
43. Osterloh, F. E., Solution Self-Assembly of Magnetic Light Modulators from Exfoliated Perovskite and Magnetite Nanoparticles. *J. Am. Chem. Soc.* **2002,** *124*, 6248-6249.
44. Tao, Q.; He, H.; Frost, R. L.; Yuan, P.; Zhu, J., Nanomaterials based upon silylated layered double hydroxides. *Appl. Surf. Sci.* **2009,** *255* (7), 4334-4340.
45. Park, A. Y.; Kwon, H.; Woo, A. J.; Kim, S. J., Layered Double Hydroxide Surface Modified with (3-aminopropyl)triethoxysilane by Covalent Bonding. *Adv. Mater.* **2005,** *17* (1), 106-109.
46. Bruzaud, S.; Levesque, G., Polysiloxane-g-TiNbO5 Nanocomposites: Synthesis via in Situ Intercalative Polymerization and Preliminary Characterization. *Chem. Mater.* **2002,** *14*, 2421-2426.
47. Ide, Y.; Ogawa, M., Surface modification of a layered alkali titanate with organosilanes. *Chem. Comm.* **2003,** (11), 1262-3.

48. Ide, Y.; Ogawa, M., Swelling Behaviors of an Organosilylated Lithium Potassium Titanate in Organic Solvents. *Chem. Lett.* **2005,** *34* (3), 360-361.
49. Ide, Y.; Ogawa, M., Preparation and som eproperties of organically modified layered alkali titanates with alkylmethoxysilanes. *J. Colloid Interface Sci.* **2006,** *296*, 141-149.
50. Nakato, T.; Hashimoto, S., Dispersion of Layered Hexaniobate in Organic Solvents through Silylation and Liquid Crystalline Behavior of the Colloidal Suspension. *Chem. Lett.* **2007,** *36* (10), 1240-1241.
51. Carroll, E. C.; Compton, O. C.; Madsen, D.; Osterloh, F. E.; Larsen, D. S., Ultrafast Carrier Dynamics in Exfoliated and Functionalized Calcium Niobate Nanosheets in Water and Methanol. *J. Phys. Chem. C* **2008,** *112*, 2394-2403.
52. Coleman, J. N.; Lotya, M.; O'Neill, A.; Bergin, S. D.; King, P. J.; Khan, U.; Young, K.; Gaucher, A.; De, S.; Smith, R. J.; Shvets, I. V.; Arora, S. K.; Stanton, G.; Kim, H. Y.; Lee, K.; Kim, G. T.; Duesberg, G. S.; Hallam, T.; Boland, J. J.; Wang, J. J.; Donegan, J. F.; Grunlan, J. C.; Moriarty, G.; Shmeliov, A.; Nicholls, R. J.; Perkins, J. M.; Grieveson, E. M.; Theuwissen, K.; McComb, D. W.; Nellist, P. D.; Nicolosi, V., Two-Dimensional Nanosheets Produced by Liquid Exfoliation of Layered Materials. *Science* **2011,** *331* (6017), 568-571.
53. Wang, X.; Xing, W.; Zhang, P.; Song, L.; Yang, H.; Hu, Y., Covalent functionalization of graphene with organosilane and its use as a reinforcement in epoxy composites. *Compos. Sci. Technol.* **2012,** *72* (6), 737-743.
54. Takahashi, S.; Nakato, T.; Hayashi, S.; Sugahara, Y.; Kuroda, K., Formation of Methoxy-Modified Interlayer Surface via the Reaction between Methanol and Layered Perovskite HLaNb2O7.cntdot.xH2O. *Inorg. Chem.* **1995,** *34* (20), 5065-9.
55. Suzuki, H.; Notsu, K.; Takeda, Y.; Sugimoto, W.; Sugahara, Y., Reactions of Alkoxyl Derivatives of a Layered Perovskite with Alcohols: Substitution Reactions on the Interlayer Surface of a Layered Perovskite. *Chem. Mater.* **2003,** *15*, 636-641.
56. Boykin, J. R.; Smith, L. J., Rapid Microwave-Assisted Grafting of Layered Perovskites with n-Alcohols. *Inorg. Chem.* **2015,** *54* (9), 4177-9.
57. Wang, Y.; Nikolopoulou, M.; Delahaye, E.; Leuvrey, C.; Leroux, F.; Rabu, P.; Rogez, G., Microwave-assisted functionalization of the Aurivillius phase Bi2SrTa2O9: diol grafting and amine insertion vs. alcohol grafting. *Chem. Sci* **2018,** *9* (35), 7104-7114.

58. Shimada, A.; Yoneyama, Y.; Tahara, S.; Mutin, P. H.; Sugahara, Y., Interlayer surface modification of the protonated ion-exchangeable layered perovskite HLaNb2O7•xH2O with organophosphonic acids. *Chem. Mater.* **2009,** *21* (18), 4155-4162.
59. Kimura, N.; Kato, Y.; Suzuki, R.; Shimada, A.; Tahara, S.; Nakato, T.; Matsukawa, K.; Mutin, P. H.; Sugahara, Y., Single- and double-layered organically modified nanosheets by selective interlayer grafting and exfoliation of layered potassium hexaniobate. *Langmuir* **2014,** *30* (4), 1169-75.
60. Suzuki, R.; Sudo, M.; Hirano, M.; Idota, N.; Kunitake, M.; Nishimi, T.; Sugahara, Y., Inorganic Janus nanosheets bearing two types of covalently bound organophosphonate groups via regioselective surface modification of K4Nb6O17.3H2O. *Chem. Comm.* **2018,** *54* (45), 5756-5759.
61. Machida, S.; Sohmiya, M.; Ide, Y.; Sugahara, Y., Solid-State (31)P Nuclear Magnetic Resonance Study of Interlayer Hydroxide Surfaces of Kaolinite Probed with an Interlayer Triethylphosphine Oxide Monolayer. *Langmuir* **2018,** *34* (43), 12694-12701.
62. Sugaya, T.; Ozaki, M.; Guegan, R.; Idota, N.; Sugahara, Y., Surface Modification of Layered Perovskite Nanosheets with a Phosphorus Coupling Reagent in a Biphasic System. *Langmuir* **2019,** *35* (20), 6594-6601.
63. Kim, D.; Ko, T. Y.; Kim, H.; Lee, G. H.; Cho, S.; Koo, C. M., Nonpolar Organic Dispersion of 2D Ti3C2Tx MXene Flakes via Simultaneous Interfacial Chemical Grafting and Phase Transfer Method. *ACS Nano* **2019,** *13* (12), 13818-13828.
64. Sugaya, T.; Guegan, R.; Idota, N.; Tsukahara, T.; Sugahara, Y., Highly Efficient Surface Modification of Layered Perovskite Nanosheets with a Phosphorus Coupling Reagent Making Use of Microchannels. *Langmuir* **2020,** *36* (26), 7252-7258.
65. Stankovich, S.; Piner, R. D.; Nguyen, S. T.; Ruoff, R. S., Synthesis and exfoliation of isocyanate-treated graphene oxide nanoplatelets. *Carbon* **2006,** *44* (15), 3342-3347.
66. Ohno, K.; Zhao, C.; Nishina, Y., Polymer-Brush-Decorated Graphene Oxide: Precision Synthesis and Liquid-Crystal Formation. *Langmuir* **2019,** *35* (33), 10900-10909.
67. Díaz, A.; Mosby, B. M.; Bakhmutov, V. I.; Martí, A. A.; Batteas, J. D.; Clearfield, A., Self-Assembled Monolayers Based Upon a Zirconium Phosphate

Platform. *Chem. Mater.* **2013,** *25* (5), 723-728.
68. Baker, J.; Xia, F.; Zhu, Z.; Zhang, X.; Sue, H. J., alpha-Zirconium Phosphate Nanoplatelets with Covalent Modifiers for Exfoliation in Organic Media. *Langmuir* **2020,** *36* (40), 11948-11956.
69. WATSON, J.; CRICK, F., Molecular Structure of Nucleic Acids - a Structure for Deoxyribose Nucleic Acid. *Nature* **1953,** *171*, 737–738.
70. Seeman, N. C., DNA in a material world. *Nature* **2003,** *421*, 427-431.
71. Rothemund, P. W. K., Folding DNA to create nanoscale shapes and patterns. *Nature* **2006,** *440*, 297-302.
72. Park, S. Y.; Lytton-Jean, A. K.; Lee, B.; Weigand, S.; Schatz, G. C.; Mirkin, C. A., DNA-programmable nanoparticle crystallization. *Nature* **2008,** *451* (7178), 553-6.
73. Dai, W.; Kumar, S. K.; Starr, F. W., Universal two-step crystallization of DNA-functionalized nanoparticles. *Soft Matter* **2010,** *6* (24), 6130–6135.
74. Zhu, C.; Zeng, Z.; Li, H.; Li, F.; Fan, C.; Zhang, H., Single-layer MoS2-based nanoprobes for homogeneous detection of biomolecules. *J. Am. Chem. Soc.* **2013,** *135* (16), 5998-6001.
75. Ge, J.; Ou, E. C.; Yu, R. Q.; Chu, X., A novel aptameric nanobiosensor based on the self-assembled DNA-MoS2 nanosheet architecture for biomolecule detection. *J. Mater. Chem. B* **2014,** *2* (6), 625-628.
76. Lin, B.; Sun, Q.; Liu, K.; Lu, D.; Fu, Y.; Xu, Z.; Zhang, W., Label-free colorimetric protein assay and logic gates design based on the self-assembly of hemin-graphene hybrid nanosheet. *Langmuir* **2014,** *30* (8), 2144-51.
77. Xu, Y.; Wu, Q.; Sun, Y.; Bai, H.; Shi, G., Three-Dimensional Self-Assembly of Graphene Oxide and DNA into Multifunctional Hydrogels. *ACS Nano* **2010,** *4*, 7358-7362.
78. Kim, T. W.; Kim, I. Y.; Park, D. H.; Choy, J. H.; Hwang, S. J., Highly Stable Nanocontainer of APTES-Anchored Layered Titanate Nanosheet for Reliable Protection/Recovery of Nucleic Acid. *Sci Rep* **2016,** *6*, 21993.
79. Tang, L.; Wang, Y.; Liu, Y.; Li, J., DNA-Directed Self-Assembly of Graphene Oxide with Applications to Ultrasensitive Oligonucleotide Assay. *ACS Nano* **2011,** *5*, 3817–3822.

Chapter 2

Grafting of Fluorescence-Labeled ssDNA onto Inorganic Nanosheets and Detection of a Target DNA

2.1 Introduction

Deoxyribonucleic acids (DNA) composed of four kinds of nucleic acid monomers, adenine (A), guanine (G), cytosine (C), and thymine (T), are known as key components that manage the genetic information of living matters through complimentary interaction of A with T and G with C to form double-stranded DNAs (dsDNAs). In addition to the importance in biotechnology and gene-therapy applications,[1] since synthetic procedure of DNAs with controlled monomer sequence is well-established, DNA-nanotechnologies are emerging as a novel research field in materials sciences, aiming at programmable nanofabrications[2, 3] and molecular computing.[4]

Combining DNAs with other kinds of nanomaterials is further promising to achieve various functional materials with precisely regulated nanostractures. For example, by using single-stranded DNA (ssDNA) as a linker of nano particles, the particles can be assembled in programmable ways. Depending on the base sequence of the linker ssDNA, gold nanoparticles were assembled into colloidal crystals with different crystal structure and lattice constants,[5,6,7] leading to different plasmon absorption that was applicable to DNA detection.[8]

Among many kinds of nanomaterials, inorganic nanosheets are focused as functional nano-modules[9] that possess very large specific surface area suitable for catalyst, adsorbent, and sensor applications. It is also recently focused that they are self-assembled into hierarchical structures such as liquid crystal phases that show intriguing optical and rheological properties.[10, 11] Hence, combining nanosheets with DNA is promising for many applications. Xu et al. reported the formation of hydrogel by heating a dsDNA/graphene mixture, leading to dehybridization of the dsDNAs to ssDNAs that crosslinked the nanosheets.[12] Tang et al. reported that the graphene nanosheets adsorbed with ssDNA detect complementary ssDNAs, resulting in the formation of graphene aggregates.[13] Zhu et al. utilized fluorescence-quenching property of MoS_2 nanosheets to detect a target ssDNA.[14] Kim et al. reported amino-modified titanate nanosheets were aggregated by addition of dsDNA.[15] Yamaguchi et al. reported liquid crystal phase formation of clay mineral nanosheet colloids is strongly enhanced by mixing with dsDNAs.[16]

However, in all of these previous reports, ssDNAs are not chemically grafted on the nanosheets but only adsorbed through physical interactions such as electrostatic interaction, hydrogen bond, and van der Waals interaction. The absence of robust

covalent bonding causes low stability of the system: e.g. physically adsorbed DNA would be easily detached in the presence of salt in a buffer solution, at higher temperature, at low pH etc. This prevents high-precision structure formation by further modification and limits advanced applications.

In this study, we succeeded in grafting ssDNAs on nanosheet surfaces and demonstrated that the grafted ssDNA undergo hybridization with complementary ssDNA, that is prerequisite for future applications such as programmable nano-fabrications using the molecular information of a DNA and gene-therapy.

We chose layered hexaniobate having modifiable hydroxy groups on the layer surface as the counterpart of the ssDNA. Chemical modification of layered silicates and transition metal oxides have been reported by many researchers so far.[17] In most cases, starting from powders of layered crystals, long chain alkylammonium is first intercalated to expand the interlayer distance and to make the interlayer space hydrophobic, allowing subsequent reaction with silylating agents in a hydrophobic solvent.[18] However, grafting with bulky molecule in high yield is difficult and it is also difficult to obtain highly exfoliated layers that is favorable for applications.

Hence, to achieve our purpose, we first prepared the colloidal sol of fully exfoliated niobate nanosheets, followed by freeze-drying the sol to obtain cotton-like voluminous solid inside which large specific surface area of the nanosheets remain exposed.[19] Then, ssDNA was grafted in three steps (Scheme 2-1). First, the Nb-OH groups on the niobate nanosheet were reacted with 3-aminopropyldiethoxymethylsilane (APDES) to form amino-functionalized niobate nanosheets. Then, the carboxy-functionalized niobate nanosheets were obtained by the subsequent reaction with succinic anhydride. Finally, fluorescence labeled amino-terminated ssDNA (FITC-ssDNA-NH_2) was attached to the carboxy-functionalized niobate nanosheets in the presence of 1-(3-dimethylaminopropyl)-3-ethylcarbodiimide hydrochloride (EDC) and *N*-hydroxysulfosuccinimide sodium salt (Sulfo-NHS) through EDC-mediated coupling reaction. The details of the synthetic procedure are described in the supporting information. Although this grafting process is well-known and has been applied to modify silica surfaces,[20, 21] it has never been applied for inorganic nanosheets or for niobate surface.

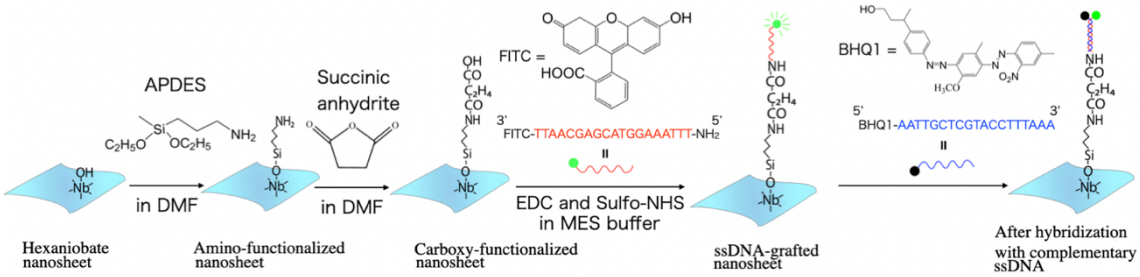

Scheme 2-1 Schematic representations of the synthesis of the ssDNA-grafted nanosheet and the detection of the target complementary ssDNA by hybridization.

2.2 Experiment

Materials Potassium carbonate, niobium oxide, *N,N*-dimethylformamide, succinic anhydride, sodium hydroxide and chloroform were purchased from Wako. *n*-propylammonium chloride, 3-aminopropyldiethoxymethylsilane, triethylamine, *N*-hydroxysulfosuccinimide sodium salt and 1-(3-dimethylaminopropyl)-3-ethylcarbodiimide hydrochloride were purchased from TCI. BHQ-1-ssDNA and FITC-ssDNA-NH_2 were purchased from Sigma-Aldrich Japan. 2-morpholinoethanesulfonic acid, monohydrate (MES) was purchased from Dojindo Laboratories. All the reagents were used as received without purification. MES buffer, was prepared by adding 0.21 g of MES in 10 ml of water, followed by adjusting pH 7.0 by addition of 0.1 mol/L of NaOH solution.

The synthesis of layered hexaniobate single crystals and preparation of colloidal sol and freeze-dried powders of hexaniobate nanosheets Mixture of potassium carbonate (9.41 g) and niobium oxide (20.58 g) powders was heated at 1423 K,and then cooled slowly to obtain $K_4Nb_6O_{17}$ single crystals, according to the method previously reported.[22] The X-ray diffraction (XRD) pattern of the powder sample obtained by grinding the crystals (Figure 2-1) was in accordance with the published data.[23] The $K_4Nb_6O_{17}$ crystals (4.44 g) were then allowed to react with an aqueous solution of *n*-propylammonium chloride (0.2 M, 200 ml) at 353 K for 7 d. The aqueous sol was centrifuged and the sediment was washed three times with deionized water, followed by dialysis against water for 3 d. The formation of fully exfoliated nanosheets with the uniform thickness of 2.0 nm and lateral size of ca. 2.0 μm was confirmed by atomic force microscopy observation (Figure 2-2). The concentration of the colloidal hexaniobate nanosheets was adjusted to 2.0 wt% by adding water and the colloid was finally freeze-

dried to obtain powdery samples.

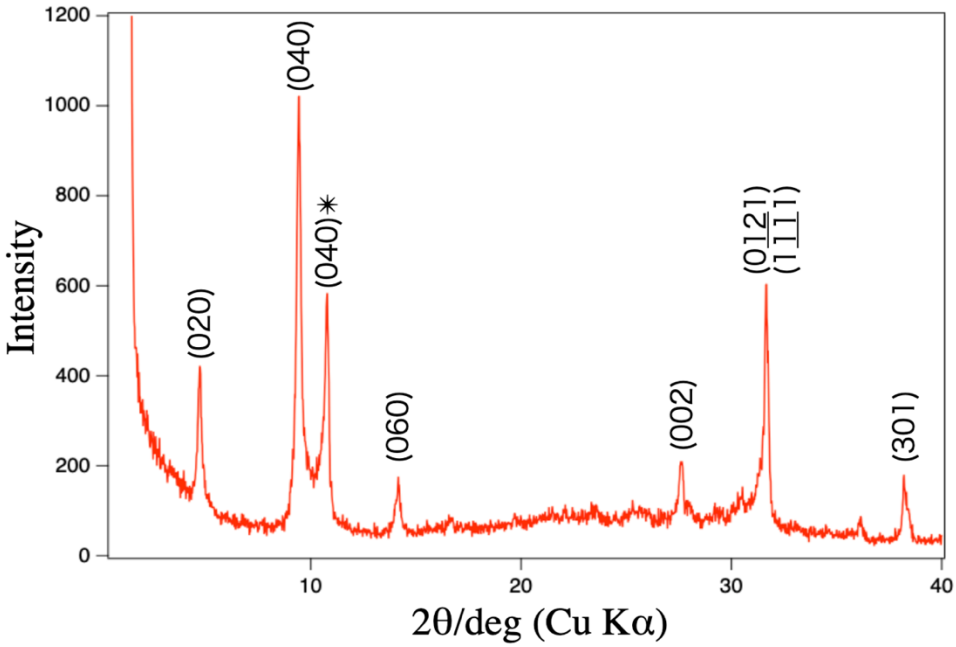

Figure 2-1 The XRD pattern of the powders of $K_4Nb_6O_{17}$. The peak marked as ✳is due to unhydrated hexaniobate ($K_4Nb_6O_{17}$) while other peaks are ascribed to tri-hydrated hexaniobate ($K_4Nb_6O_{17}$・$3H_2O$).

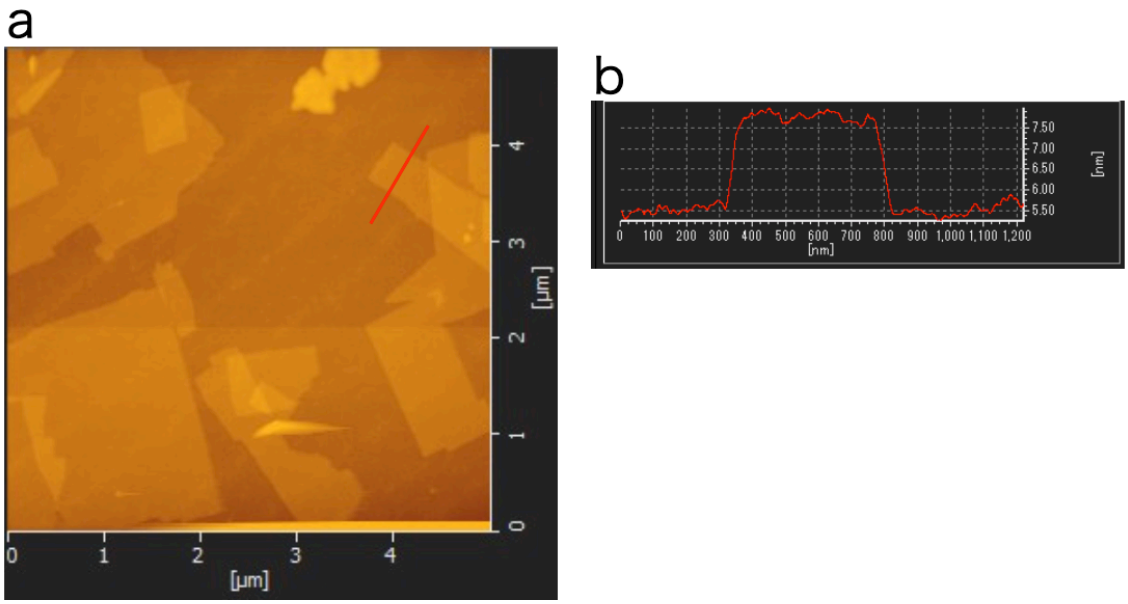

Figure 2-2 AFM image of the hexaniobate nanosheet (a) and its cross section profile (b).

Grafting ssDNAs on the niobate layers ssDNA-grafted nanosheets were synthesized in four steps. First, amino-functionalized nanosheets were obtained by stirring the freeze dried nanosheets (0.02 mmol) in the mixture of *N,N*-

dimethylformamide (30 ml), triethylamine (0.1 mmol), and 3-aminopropyldiethoxymethylsilane (2.0 mmol) at 130 ºC for 24 h, followed by filtration and washing with chloroform. Then, carboxy-functionalized nanosheets were obtained by stirring 0.1 g of the amino-functionalized nanosheets in the mixture of *N,N*-dimethylformamide (25 mL), triethylamine (0.43 g) and succinic anhydride (0.85 g) at room temperature for 8 h, followed by filtration and washing with chloroform. Finally, 0.05 g of carboxy-functionalized nanosheets were stirred at room temperature for 6 h in 5 ml of MES buffer (pH 7.0) added with 50 mg of 1-(3-dimethylaminopropyl)-3-ethylcarbodiimide hydrochloride (EDC), 50 mg of *N*-hydroxysulfosuccinimide sodium salt (Sulfo-NHS), and 50 μL of the aqueous solution of 100 μM ssDNA having an amino group and fluorescent moiety (FITC) at the 5' and 3' ends, respectively, followed by filtration and washing with pure water.

Hybridization test of ssDNAs-grafted nanosheets with the complementary ssDNA FITC-ssDNA-grafted samples were dispersed in water and the concentration was adjusted to 0.5 wt%. Then, 100 μL of this dispersion was added with 5 μL of 100 μM aqueous solution of complementary ssDNA with the quencher molecule BHQ-1 at the 5' end and observed by confocal laser scanning microscopy (CLSM) at room temperature.

Characterization Infrared (IR) spectra were recorded on a Agilent Technologies Cary 670 using the KBr disk method. X-ray diffraction (XRD) patterns were obtained with a Shimazu XRD 7000L (Cu Kα radiation) diffractometer. Confocal laser scanning microscopy observations (CLSM) were conducted with a Nikon A1R+ in the back-scattering mode using the 405 nm diode laser and no filter as well as in the fluorescence mode using the 488 nm Ar laser and the emission filter with the maximum transmission wavelength of 525 nm.

2.3 Result and Discussion

The grafting of the ssDNA was first confirmed by infrared (IR) spectra (Figure 2-3). Before modification (Figure 1a), the bands due to Nb-O (500-906 cm^{-1}) (●) and N-H (amine) (1648 cm^{-1}) (■) of the exfoliating agent, *n*-propylammonium, are observable. After the reaction of the nanosheets with APDES (Figure 2-3b), the band due to Si-O-C stretching vibration appears at 1080 cm^{-1}(☆), while peaks due to the N-H bending vibration (amine) (1648 cm^{-1}) (■) and C-N stretching vibration (1250 cm^{-1}) (▲) are stronger than before modification (Figure 3a), indicating grafting of APDES. After the

subsequent reaction of the APDES-modified nanosheets with succinic anhydride (Figure 2-3c), C=O stretching vibration appears at 1700 cm^{-1}(△), in addition to the broad N-H (amido) bending vibration band at 1650 cm^{-1} (■). These results indicated that the carboxy-functionalized nanosheet was obtained through the condensation of the amino group on the nanosheets with succinic anhydride, forming amide bonds. After the reaction with FITC-ssDNA-NH_2 (Figure 2-3d), the strong bands due to DNA (◇) are observed: the stretching vibrations of P=O (1180 cm^{-1}), C-H (aromatic) (3020 cm^{-1}), C=C (1504 cm^{-1}) and C=N (pyrimidine base) (1569 cm^{-1}).

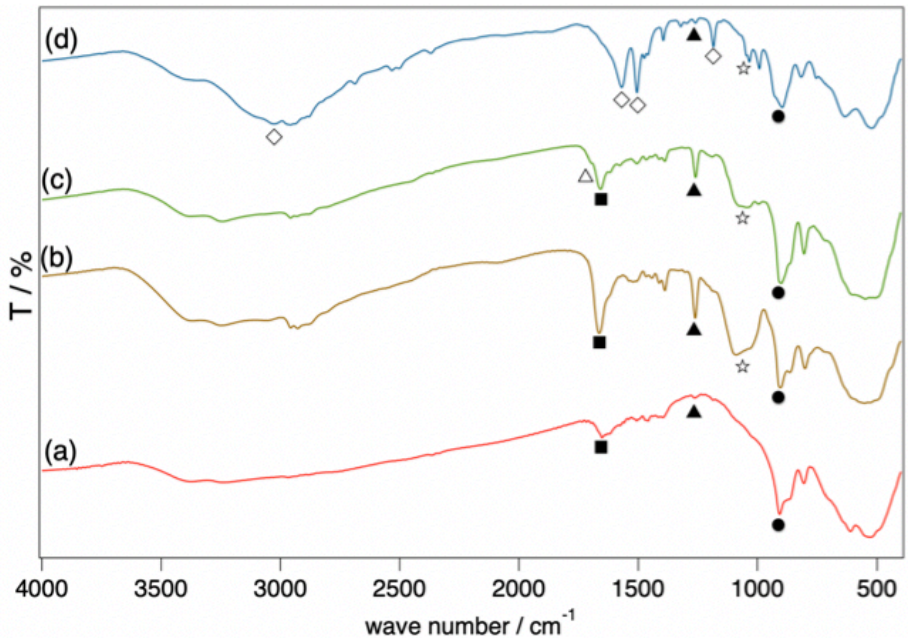

Figure 2-3 IR spectra of (a) the hexaniobate nanosheets before modification, (b) amino-functionalized nanosheets, (c) carboxy-functionalized nanosheets, and (d) FITC-ssDNA-NH2-grafted nanosheets.

The X-ray diffraction (XRD) measurements of the dried powder samples also confirmed the modification of the niobate layers. Before modification (Figure 2-4a), the peaks are observed at d = 2.1 and 1.0 nm, which are ascribed to the *n*-propylammonium-intercalated hexaniobate,[24] considering the thickness of the niobate layer of 1.7 nm and the molecular size of the *n*-propylammonium, 0.4 nm. The *d*-value did not change after grafting APDES (Figure 2-4b) because the molecular size of APDES is similar to *n*-

propylammonium. After the reaction with succinic anhydride, the basal spacing increased to 2.6 nm, which increment mostly matches the length of the attached -CO-C_2H_4-COOH group. By reaction with FITC-ssDNA-NH_2 (Figure 2-4d), the basal spacing further increases to 3.2 nm, that corresponds to the gallery height of 1.5 nm, confirming the modification with bulkier components. The radius of gyration R_g of Gaussian chain of ssDNA is calculated as $R_g = A_0 N^{\nu}$, where A_0 (~ 0.6-0.7) is the scaling prefactor, ν (~ 0.3) is the scaling exponent[25] and N (=19) is the number of the monomer units in the DNA chain used in this study; the R_g is roughly calculated as 1.7-2.4 nm. Meanwhile, the molecular thickness of a FITC and ssDNA are both ca. 1 nm. Thus, the observed basal spacing is compatible with the size of the modified components, although configuration of the modified ssDNA is unknown.

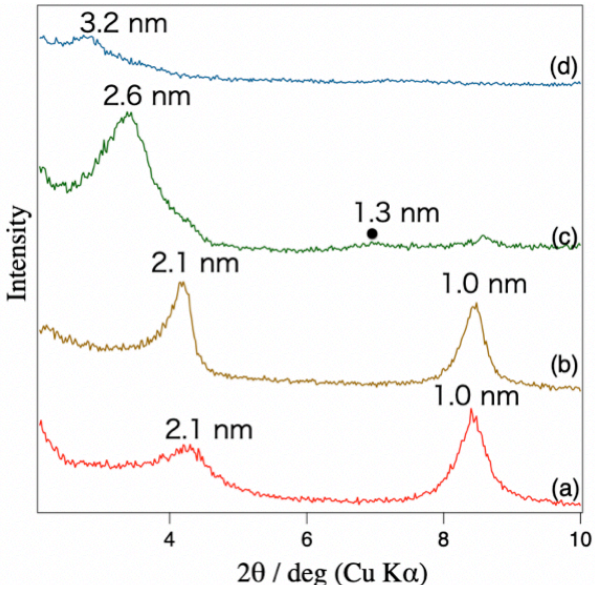

Figure 2-4 XRD patterns of (a) the hexaniobate nanosheets before modification, (b) amino-functionalized nanosheets, (c) carboxy-functionalized nanosheets, and (d) FITC-ssDNA-NH2-grafted nanosheets.

The grafting of the ssDNAs on the nanosheets was further confirmed by the observations by confocal laser scanning microscopy (CLSM) (Figure 2-5). In the scattering image of FITC-ssDNA-NH_2-grafted nanosheets (Figure 2-5b), the particles with the size of several tens of μm are observed. Considering the average size of the nanosheets (ca. 2 μm, Figure 2-2), the particles are the aggregates of nanosheets formed during the freeze-dry process. Importantly, the fluorescence image (Figure 2-5e) is similar to the scattering image, indicating that the fluorescent FITC is present on the

niobate nanosheets. In contrast, in the case of the nanosheets before modification, the particles are only observed in the scattering image (Figure 2-5a) and not in the fluorescence image (Figure 2-5d). Fluorescence was neither observed in the sample prepared by the reaction of FITC-ssDNA-NH_2 with the nanosheets, instead of carboxy-functionalized one (Figure 2-5c, f). We also confirmed that the fluorescence is not observed when the reaction of FITC-ssDNA-NH_2 with carboxy-functionalized was conducted without EDC and Sulfo-NHS (Figure 2-6). These results confirm that the ssDNA was stably immobilized on the nanosheet through covalent bond, not by weak interaction such as van der Waals force, electrostatic interaction, and hydrogen bond between the terminal amino group on the ssDNA and the NbO^- or -COOH group on the nanosheets. We further confirmed that the grafted ssDNA was stably held even under an acidic condition (Figure 2-7), in which condition electrostatically modified FITC-DNA-NH_2 should have been easily detached. The robust modification of DNA on the nanosheet is the strong merit of the present study that allows wide range of applications.

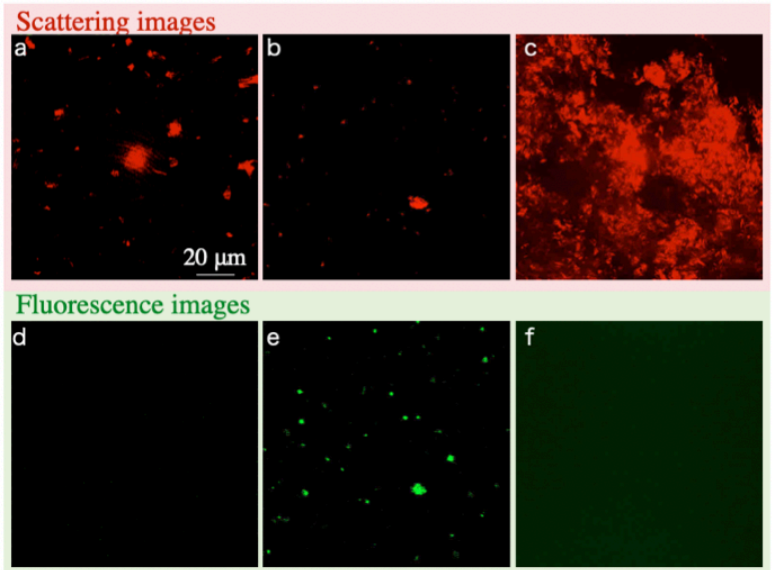

Figure 2-5 CLSM images of (a)(d) the hexaniobate nanosheets before modification, (b)(e) FITC-ssDNA-NH2-grafted nanosheets, and (c)(f) the control sample obtained by simply mixing FITC-ssDNA-NH2 and the nanosheets, followed by washing in the same condition as (b). (a)-(c) are the scattering mode images. (d)-(f) are the fluorescence images observed with the excitation and emission wavelengths of 405 and 488 nm, respectively, to detect FITC.

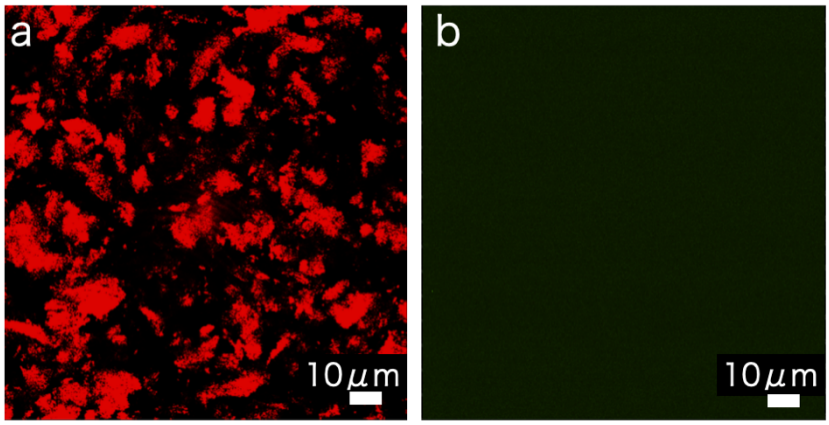

Figure 2-6 CLSM observation in the (a) scattering mode and (b) fluorescence mode of the sample prepared by the reaction of the carboxy-functionalized nanosheets with FITC-ssDNA-NH2 without EDC and Sulfo-NHS. The carboxy-functionalized nanosheets (0.05 g) were added with 5 ml of MES buffer (pH 7.0) and 50 μL of the aqueous solution of 100 μM FITC-ssDNA-NH2, followed by stirring at room temperature for 6 h, infiltration, and washing with pure water.

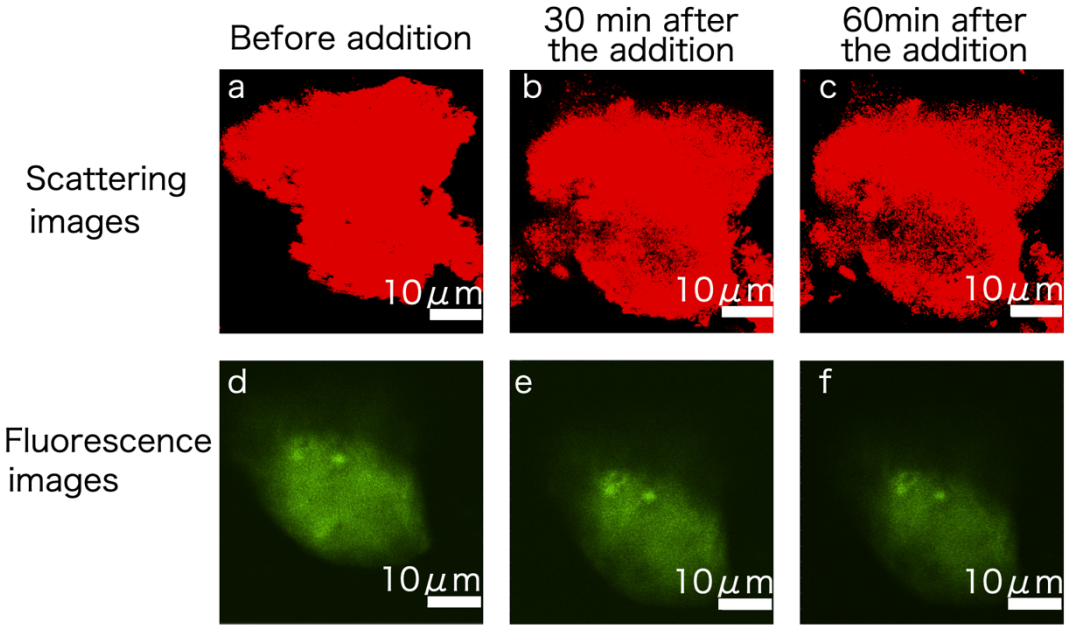

Figure 2-7 CLSM images in the (a-c) scattering and (d-f) fluorescence modes (a)(d) before and (b)-(f) after addition of 0.1 mL of 1×10^{-3} M HCl aq to the 0.1 mL of the colloidal sol of the ssDNA-grafted nanosheets. This observation confirms that the fluorescent labeled ssDNA is stably held even under the acidic condition at least for 60 min.

We finally examined if the expected hybridization reaction of the grafted ssDNA proceeds with a complementary ssDNA even in the situation that the motion of the ssDNA chains and access to the ssDNA are restricted in the interlayer or on the surface of the niobate nanosheets. As shown in the CLSM images (Figure 2-8), initially observed fluorescence on the particles gradually disappears after addition of complementary ssDNA terminated with the quencher molecule BHQ-1 (the base sequences of each ssDNA are shown in Scheme 1). Finally, after 15 min, the fluorescence completely disappeared. The fluorescence quenching is known to take place only when the quencher and the fluorescent molecules are present in the close distance for fluorescence resonance energy transfer, the situation which only occurs when expected hybridization reaction proceeds. Thus, the detection of the target ssDNA through hybridization with the ssDNA on the nanosheets was confirmed.

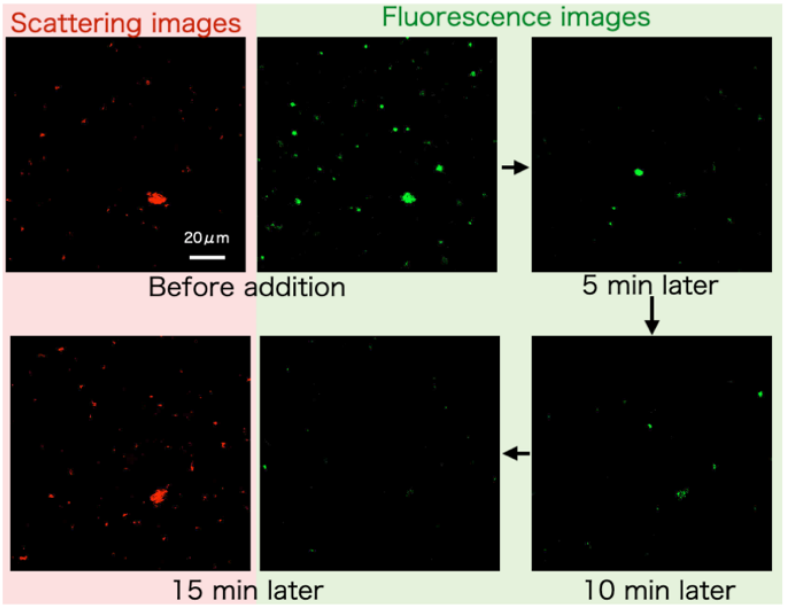

Figure 2-8 Time-course of the CLSM images of the FITC-ssDNA-NH2- grafted nanosheets before and after adding the complementary BHQ1-ssDNA.

2.4 Conclusion

A functional biomolecule, ssDNA was for the first time grafted on an inorganic nanosheet and the grafted ssDNAs were confirmed to undergo hybridization reaction with the ssDNA with complementary base sequence, resulting in detection of a target ssDNA through fluorescence quenching. The present system will be applicable for programmable nano-fabrications, DNA-based molecular robotics,[26] and gene therapy.[1]

2.5 References

1. Cabral, H.; Miyata, K.; Osada, K.; Kataoka, K., Block Copolymer Micelles in Nanomedicine Applications. *Chem. Rev.* **2018,** *118* (14), 6844-6892.

2. Seeman, N. C., DNA in a material world. *Nature* **2003,** *421*, 427-431.

3. Rothemund, P. W. K., Folding DNA to create nanoscale shapes and patterns. *Nature* **2006,** *440*, 297-302.

4. M. N. Stojanovic; Mitchell, T. E.; Stefanovic, D., Deoxyribozyme-Based Logic Gates. *J. Am. Chem. Soc.* **2002,** *124*, 3555-3561.

5. Park, S. Y.; Lytton-Jean, A. K.; Lee, B.; Weigand, S.; Schatz, G. C.; Mirkin, C. A., DNA-programmable nanoparticle crystallization. *Nature* **2008,** *451* (7178), 553-6.

6. Dai, W.; Kumar, S. K.; Starr, F. W., Universal two-step crystallization of DNA-functionalized nanoparticles. *Soft Matter* **2010,** *6* (24), 6130–6135.

7. Lara, F. V.; Starr, F. W., Stability of DNA-linked nanoparticle crystals I: Effect of linker sequence and length. *Soft Matter* **2011,** *7* (5), 2085–2093

8. Vial, S.; Nykypanchuk, D.; Deepak, F. L.; Prado, M.; Gangb, O., Plasmonic Response of DNA-Assembled Gold Nanorods:Effect of DNA Linker Length, Temperature and Linker/Nanoparticles Ratio. *J. Colloid Interface Sci.* **2014,** *433*, 34-42.

9. Osada, M.; Sasaki, T., Two-Dimensional Dielectric Nanosheets: Novel Nanoelectronics From Nanocrystal Building Blocks. *Adv. Mater.* **2012,** *24*, 210-228.

10. Gabriel, J. C. P.; Camerel, F.; Lemaire, B. J.; Desvaux, H.; Davidson, P.; Batail, P., Swollen liquid-crystalline lamellar phase based on extended solid-like sheet. *Nature* **2001,** *413*, 504-508.

11. Miyamoto, N.; Nakato, T., Liquid crystalline nature of $K_4Nb_6O_{17}$ nanosheet sols and their macroscopic alignment. *Adv. Mater.* **2002,** *14* (18), 1267-1270.

12. Xu, Y.; Wu, Q.; Sun, Y.; Bai, H.; Shi, G., Three-Dimensional Self-Assembly of
Graphene Oxide and DNA into
Multifunctional Hydrogels. *ACS Nano* **2010,** *4*, 7358-7362.

13. Tang, L.; Wang, Y.; Liu, Y.; Li, J., DNA-Directed Self-Assembly of

Graphene Oxide with Applications to
Ultrasensitive Oligonucleotide Assay. *ACS Nano* **2011,** *5*, 3817–3822.
14. Zhu, C.; Zeng, Z.; Li, H.; Li, F.; Fan, C.; Zhang, H., Single-layer MoS2-based nanoprobes for homogeneous detection of biomolecules. *J. Am. Chem. Soc.* **2013,** *135* (16), 5998-6001.
15. Kim, T. W.; Kim, I. Y.; Park, D. H.; Choy, J. H.; Hwang, S. J., Highly Stable Nanocontainer of APTES-Anchored Layered Titanate Nanosheet for Reliable Protection/Recovery of Nucleic Acid. *Sci Rep* **2016,** *6*, 21993.
16. Yamguchi, N.; Anraku, S.; Paineau, E.; Safinya, C. R.; Davidson, P.; Michot, L. J.; Miyamoto, N., Swelling Inhibition of Liquid Crystalline Colloidal Montmorillonite and Beidellite Clays by DNA. *Sci. Rep.* **2018,** *8* (4367).
17. E.Ruiz-Hitzky; J.M.Rojo, Intracrystalline grafting on layer silicic acids. *Nature* **1980,** *287*, 28-30.
18. Okutomo, S.; Kuroda, K.; Ogawa, M., Preparation and characterization of silylated-magadiites. *Appl. Clay Sci.* **1999,** *15*, 253–264.
19. Sasaki, T.; Nakano, S.; Yamauchi, S.; Watanabe, M., Fabrication of titanium dioxide thin flakes and their porous aggregate. *Chem. Mater.* **1997,** *9*, 602-608.
20. Chen, C.; Pu, F.; Huang, Z.; Liu, Z.; Ren, J.; Qu, X., Stimuli-responsive controlled-release system using quadruplex DNA-capped silica nanocontainers. *Nucleic Acids Res.* **2011,** *39* (4), 1638-44.
21. Zhu, Y. T.; Ren, X. Y.; Liu, Y. M.; Wei, Y.; Qing, L. S.; Liao, X., Covalent immobilization of porcine pancreatic lipase on carboxyl-activated magnetic nanoparticles: characterization and application for enzymatic inhibition assays. *Mater. Sci. Eng. C* **2014,** *38*, 278-85.
22. Miyamoto, N.; Nakato, T., Liquid crystalline colloidal system obtained by mixing niobate and aluminosilicate nanosheets: a spectroscopic study using a probe dye. *Langmuir* **2003,** *19*, 8057-8064.
23. Sim, A. Y. L.; Lipfert, J.; Herschlag, D.; Doniach, S., Salt dependence of the radius of gyration and flexibility of single-stranded DNA in solution probed by small-angle x-ray scattering. *Phys. Rev. E* **2012,** *86* (2 Pt 1),

021901.
24. Murata, S.; Konagaya, A.; Kobayashi, S.; Saito, H.; Hagiiya, M., Molecular Robotics: A New Paradigm for Artifacts. *New Gener Comput* **2013,** *31*, 27-45.

Chapter 3

Modification of PMMA onto hexaniobate nanosheets maintaining dispersed state in a mixture solvent of water/DMF

3.1 Introduction

Functionalization of inorganic nanoparticles by surface modification has been investigated by many researchers and attracting attention in various research fields such as colloid science, material engineering and soft material. Modified particles have the properties such as stable dispersibility in hydrophobic solvent[1] and stimulus-responsiveness.[2]

While surface modification was mostly reported for spherical and irregularly shape particles, modification of anisotropic particles is intriguing. Among them, inorganic nanosheet with a thickness of 1 nm and a maximum width of several hundred $\mu m^3$are obtained by exfoliation of inorganic layered material such as graphite, layered clay mineral and layered silicate, in a solution. Owing to the large specific surface area and extremely anisotropic morphology as well as electrical and optical properties, nanosheets are applicable for adsorbent, catalyst, optical devices, etc. The formation of liquid crystal phase with birefringence and structural colors in colloidal state is also recently highlighted. Ruiz-Hitzky et al. firstly reported modification of silane coupling agents on the layered silicate H-magadiite.[3] Surface modification of other layered crystals having hydroxyl group on the interlayer surface such as layered silicate, layered titanite, layered niobite, graphene oxide was reported. The modified layered materials are useful as adsorbent of particular molecule[4] and show improvement in dispersion in hydrophobic solvent.[4] A few studies of preparing surface modified single-layer nanosheet have also been reported; however, in the conventional methods, the interlayer surfaces of layered crystal is first modified, followed by exfoliation by sonication, resulting in low exfoliation degree and unstable dispersion.[5, 6] It is also a problem that bulky species such as polymers and biomolecules is not easily modifiable.

In this context, direct modification to fully-exfoliated single-layer nanosheets is strongly desired. However, since most of single-layer nanosheets are stably dispersed in water, general grafting reactions such as silylation performed in hydrophobic organic solution is difficult to be applied for single-layer nanosheets. Grafting of single layer graphene oxides have been reported by several research groups taking advantage of the reactive carboxyl and epoxy groups and high dispersibility in water and N,N-dimethylformamide.[7-9] However, the structural regularity of graphene oxide is very low and this method is not applicable for other nanosheet materials except for graphene oxide. Recently, Sugaya et al. reported that highly crystalline single-layer perovskite nanosheet

was modified with oleyl phosphate in water/cyclohexane biphasic system.[10] Kim et al. also reported that exfoliated MXene was modified by oleyl phosphate in water/chloroform biphasic system.[11] However, the single-layer nanosheets were partly restacked and aggregated during the reaction. Thus, versatile synthetic procedure for direct modification of pre-exfoliated single-layer nanosheets is still to be investigated.

In this study, we report successful modification of 3-methacryloxypropylmethyl dimethoxysilane (MPDMS) onto fully-exfoliated double-layer hexaniobate nanosheets, retaining the fully exfoliated state. The MPDMS-modified nanosheet is demonstrated as superior starting material for further functionalization of the nanosheets owing to the good dispersibility in hydrophobic solvents and reactive site on MPDMS. Polymethylmethacrylate(PMMA)-modified nanosheet was finally synthesized by polymerization of MMA starting from MPDMS on the nanosheet. The modified nanosheets showed good dispersibility in hydrophobic solvents and liquid

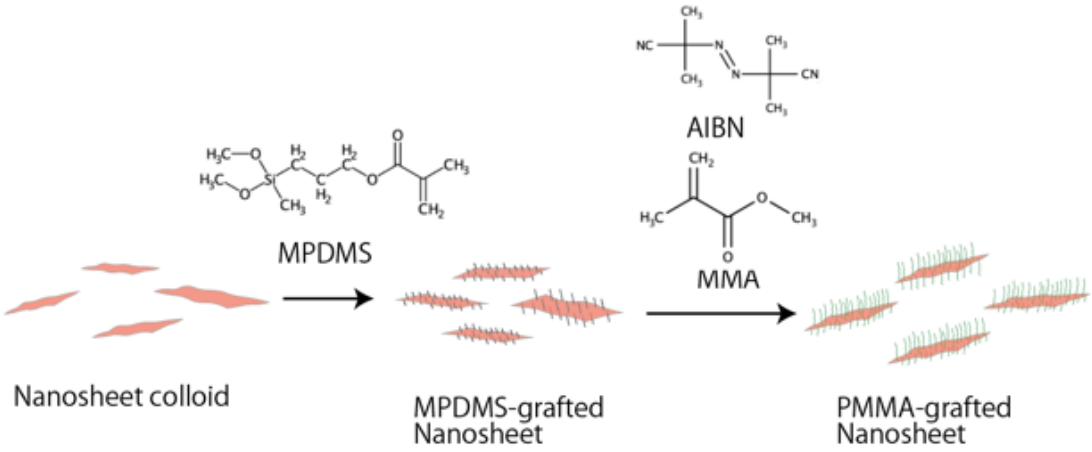

Scheme 3-1 Schematic representations of PMMA-grafted nanosheet

crystallinity.(Scheme 3-1)

Before starting the explanation of experimental results, let us introduce the unusual structural feature of the layered hexaniobate used in the present study. Layered hexaniobate has two kinds of alternating interlayers called interlayer I and II. The interlayer I is more reactive for ion-exchange and more easily swollen with water, whereas the cations in the interlayer II is difficult to be exchanged. Therefore, in a mild condition as in the present study, the hexaniobate is exfoliated uniformly as double-layer that sandwich K+ in the interlayer II. This peculiar feature originates from asymmetric

crystal structure of the layer itself. As shown in Figure 3-1, the layer surface I facing to the interlayer I has only one Nb-O- sites per a unit, whereas the Layer Surface II facing to the interlayer II has two Nb-O- sites per a unit. Therefore, the two K+ per a unit in the interlayer II are more strongly bound by the layers. Two K+ per a unit are present also in the interlayer I but only one of them is bound to NbO- on the layer surface while the other is weakly bound by the charge spread over the layer. In the condition of present study, only one NbO- group per a unit of [Nb_6O_{17}] on the Layer Surface I can be chemically modifiable.

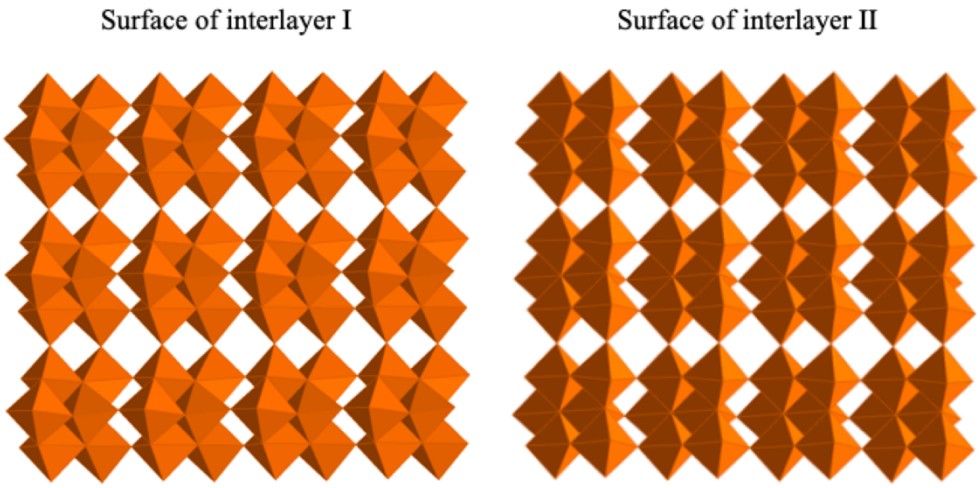

Figure 3-1 Crystal structure of hexaniobate interlayer Ⅰ interlayer Ⅱ.

3.2 Experimental

Material. Potassium carbonate, niobium oxide and *N,N*-dimethylformamide (DMF) were purchased from Wako. *n*-propylammonium chloride, 3-methacryloxypropylmethyldimethoxysilane (MPDMS) and 2,2'-azobis(isobutyronitrile) were purchased from TCI and used as received without purification. Methyl methacrylate (MMA) was purchased from TCI used after removal of polymeriation inhibiter by the treatment with activated alumina.

The synthesis of layered hexaniobate single crystals and preparation of colloidal sol. Mixture of potassium carbonate (9.41 g) and niobium oxide (20.58 g) powders was heated at 1423 K, and then cooled slowly to obtain $K_4Nb_6O_{17}$ single crystals, according to the method previously reported.[3] The $K_4Nb_6O_{17}$ crystals (4.44 g) were then allowed to react with an aqueous solution of *n*-propylammonium chloride (0.2 M, 200 ml) at 353 K for 7 d. The aqueous sol was centrifuged and the sediment was washed three

times with deionized water, followed by dialysis against water for 3 d.

Modification of MPDMS onto nanosheet. Nanosheet colloid (8 wt% , 0.3 g) was added with DMF (29.7 mL) with stirring and then added with MPDMS (0.03 g), followed by refluxing under nitrogen atmosphere at 100℃ for 3 to 7 days. After the reaction, the sample was centrifuged at 12000 rpm for 20 min. The supernatant was removed and the concentrated colloidal sol was added with 30 mL of water or DMF and centrifuged under same condition; this washing process was repeated three times.

Polymerization of MMA from MPDMS modified nanosheet. Colloidal sol of MPDMS-modified nanosheet dispersed in DMF (0.01 wt%, 28.4 g) was added with MMA (1.5 mL) and 0.008 g of 2,2'-azobis(isobutyronitrile) of 0.008 g, followed by the reaction under nitrogen atmosphere at 80 ℃ for 48 h. The obtained colloidal sol sample was centrifuged at 12000 rpm for 20 min. The supernatant was removed and the concentrated colloidal sol was added with 30 mL of DMF and centrifuged again under the same condition. This washing process was repeated three times.

Characterization. Fourier transform infrared (FTIR) spectra were recorded on a Agilent Technologies Cary 670 using a KBr disk method. Atomic force microscope was observed using an AFM5000II (Hitachi High-tech Science). Inductivity coupled plasma optical emission spectrometer (ICP-OES) was measured on a Shimadzu ICPE-9000 by the internal standard method. For this measurement, the dried colloidal sol samples was added to 20 mL of HF and heated at 200 ℃ overnight, followed by addition of 1 mL of H_2SO_4 and 0.5 mL of HNO_3 and heating at 200 ℃ for 3 h, to completely dissolve the sample. Polarized optical microscope observation was performed on a Olympus BX-51. Small-angle X -ray scattering was measured on a Rigaku NANOPIX with Cu Kα radiation at 30 V and 40 mA.

3.3 Results and Discussion

Figure 3-2 shows crossed-polarizer observation and AFM images of the samples before and after the reaction. Before the reaction (Figure 3-2a), the solution showed birefringence due to liquid crystal phase. In the AFM image (Figure 3-2 b, c), nanosheets with the lateral size of several μm and uniform thickness of 2 nm are observed. The thickness of 2 nm is compatible with the crystallographically induced thickness if tge double-layer nanosheets that sandwich K+ in the interlayer II. No obvious change in these observations is found after the reaction with MPDMS (Figure 3-2d-f), indicating that fully

exfoliated state of the single-layer nanosheets is retained.

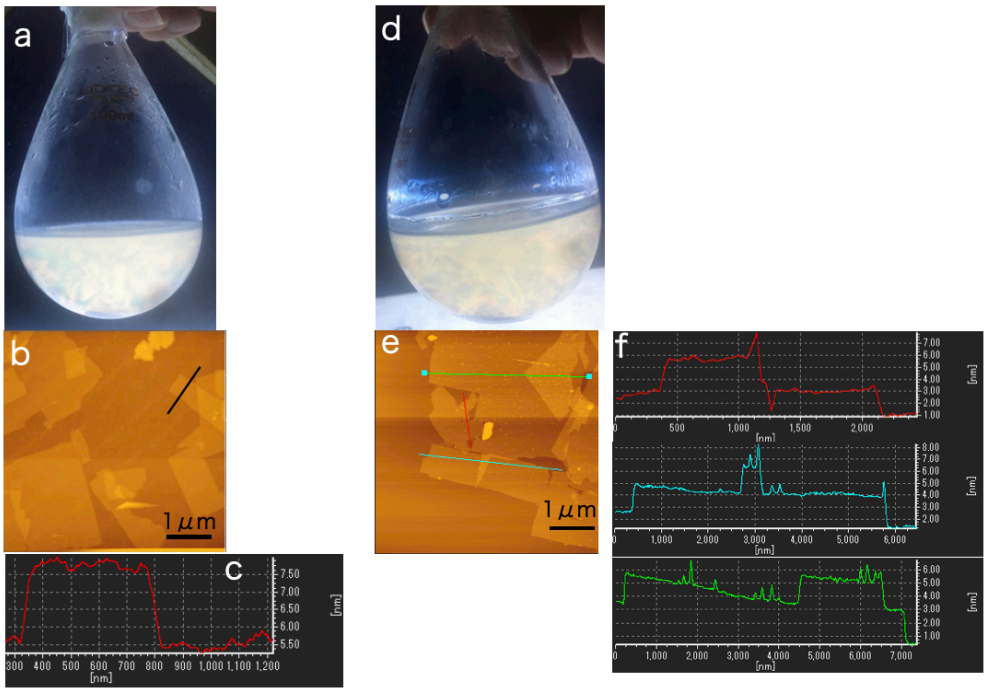

Figure 3-2 Before reaction of nanosheet colloid dispersed in mixture solvent of water/DMF (a-c), after reaction for 3 days of nanosheet colloid dispersed in mixture solvent of water/DMF (d-f), Observation of reaction solution in cross nicoles (a and d), (c and f)

The grafting of the MPDMS was confirmed by FTIR spectra (Figure 3-3). Before modification (Figure 3-3a), the bands due to Nb-O-Nb vibration (500-906 cm^{-1}) of the niobate crystal as well as C-N stretching vibration (1250 cm^{-1}; ◆), C-H(bending vibration 1460 cm^{-1}; ▲), N-H bending vibration (amine) (1648 cm^{-1}; ■) and C-H stretching vibration (2918 and 2839 cm^{-1}) of the exfoliating agent, *n*-propylammonium, are observable. After the reaction with MPDMS for 3 d (Figure 3-3b) , the bands due to Nb-O-Si stretching vibration (980 cm^{-1}; □), Si-O-Si stretching vibration (1020 cm^{-1}; ◇), Si-CH stretching vibration (1280 cm^{-1}; ■), C=O bending vibration (1480 cm^{-1}; △) and C=O stretching vibration (1700 cm^{-1}; ○) appeared. No further change is observed after the reaction for 5 and 7 d.

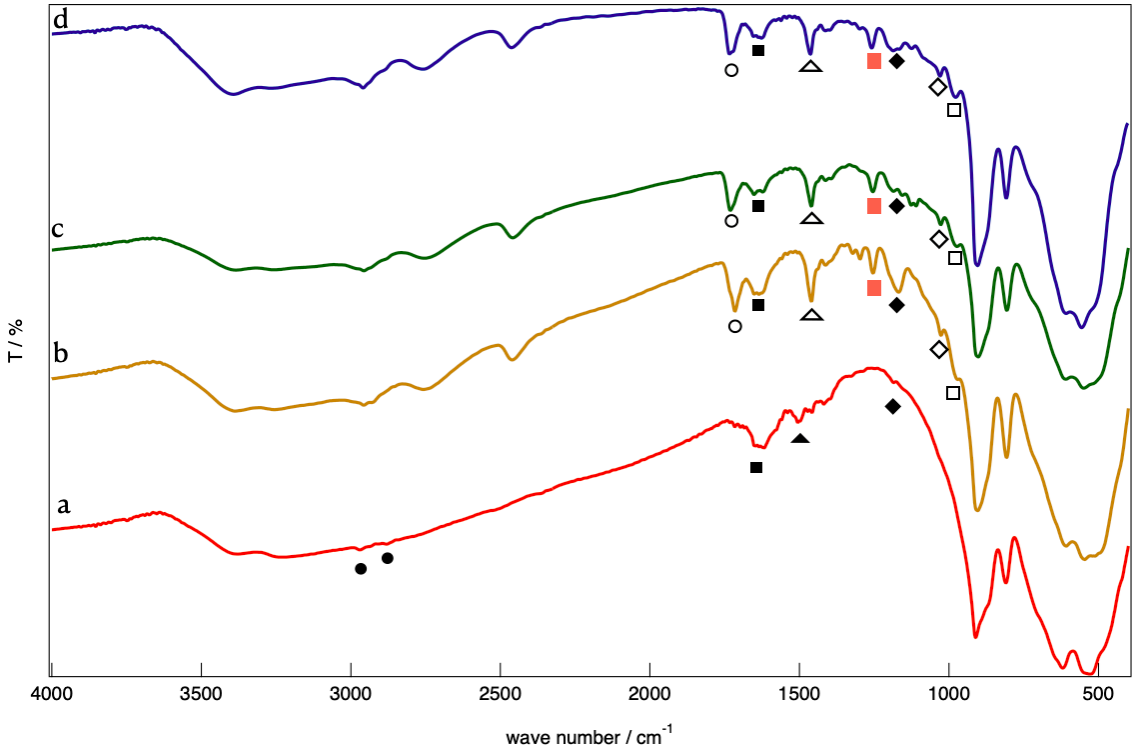

Figure 3-3 IR spectra of (a) the hexaniobate nanosheets before modification, MPDMS modified nanosheet reacted for (b) 3 days, (c) 5 days and (d) 7 days.

The WAXS measurements of dried powder samples also confirmed the modification of the niobite layers. Before modification (Figure 3-4a), the peaks are observed at d = 1.93 and 0.94 nm, which are ascribed to the *n*-propylammonium-intercalated hexaniobate, considering the thickness of the niobate layer of 1.70 nm and the molecular size of the *n*-propylammonium, 0.30 nm. The basal spacing of MPDMS modified nanosheet reacted for 3 d increased to 2.35 nm (Figure 3-4b). The basal spacing further increased to 2.44 and 2.56 nm by extending the reaction time to 5 and 7 d. Also, reaction temperature is important. The largest basal spacing *d* was obtained in the reaction time 3d at 120℃. However, basal spacing d decreases in the reaction time 3d at 140℃.

The change in the basal spacing can be explained by the difference in modified amount of MPDMS on the surface I and the amount of retained K+ in the interlayer II. According to the ICP analysis (Table 3-1), the 6.3% of the NbO- group on surface I is grafted with MPDMS when reacted for 3 d at 100 ℃, while 86% of the K+ (1.72 of 2) is retained in the interlayer II. Further increase in the d-value with the reaction for 3 d at 120 ℃ is attributed to the increase in the grafting ratio to 7.6%, while still retaining the 13% of K+ in the interlayer II. In the sample after the reaction for 5d at 100 C and for 3d

at 140 C, only 3.5-4 % of K+ is retained that can result in the compression of the interlayer II although the grafting ratio increases up to 9.1 %.

Surface coverage of MPDMS on the nanosheet is calculated based on the unit area per a unit of Nb_6O_{17} (0.783 nm x 0.646 nm = 0.506 nm^2) and the area occupied by one MPDMS molecule in a flat configuration (ca. 0.5 nm). Considering the grafting ratio,the coverage is calculated as up to 9.1% the sample reacted for 3d at 120 C. Thus, we expect higher grafting ratio by future optimization of the reaction condition.

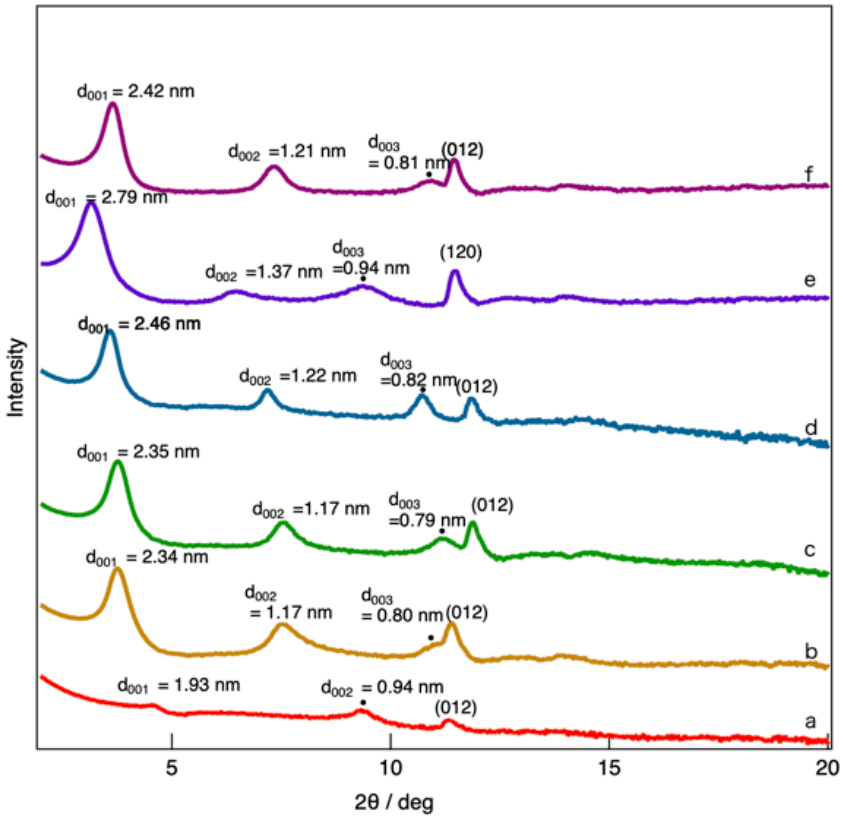

Figure 3-4 WAXS profile of the hexaniobate nanosheets (a) before modification and after the modification with MPDMS by the reaction for (b) 3 , (c) 5 and (d) 7 d at 100°C, (e) 3 d at 120°C, (f) 3 d at 140°C.

Table 3-1 Atomic ratios in the MPDMS modified nanosheet

	Atomic rate			Modification rate (%)*	Coverage (%)**
	K	Si	Nb		
3d, 100°C	1.72	0.06	6	6.3	2.4
5d, 100°C	0.07	0.07	6	7.7	3.0
3d,120°C	0.26	0.07	6	7.6	3.0
3d, 140°C	0.08	0.09	6	9.1	3.5

* The molar ratio of MPDMS to the modifiable NbO- group in Nb_6O_{17} unit of the double layer nanosheet

** The surface coverage of the MPDMS on the Layer Surface I

MPDMS modified nanosheets reacted for 3 d was dispersed in DMF and water. The colloids were observed by POM (Figure 3-5). The 3 wt% colloid of MPDMS modified nanosheet in the water showed permanent birefringence and was dispersed without aggregation. When the colloid concentration was lowered, birefringence gradually weakened. Even after exchange of the solvent from water to DMF, the birefringence and dispersed state were retained.

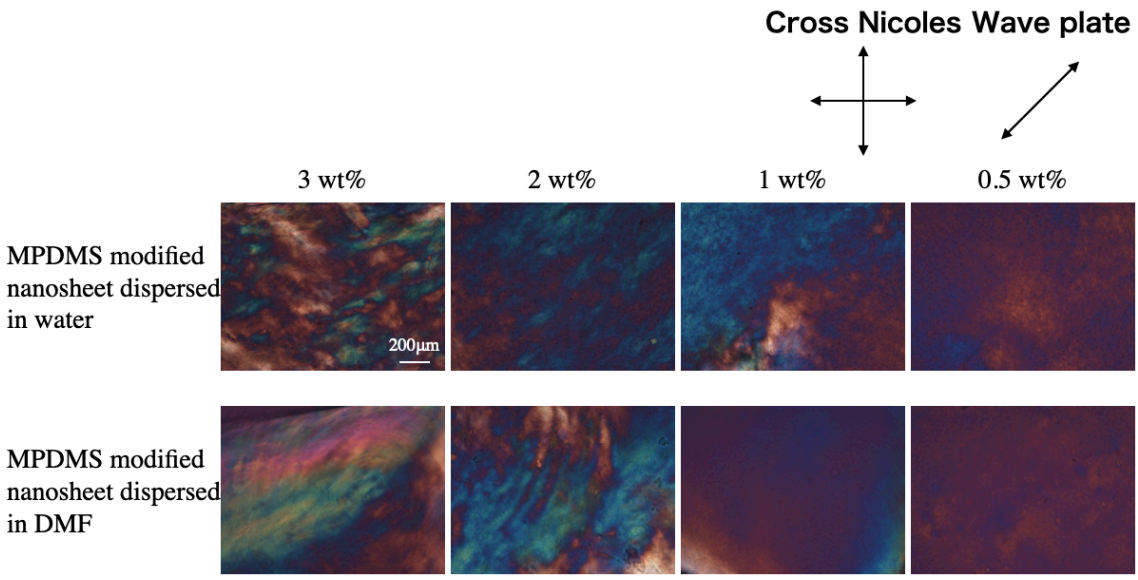

Figure 3-5 POM observation of MPDMS modified nanosheet dispersed in water and DMF.

These samples were observed with SAXS (Figure 3-6). The 3 wt% and 2wt% aqueous colloidal sol of MPDMS modified nanosheets showed the peaks due to structures with the basal spacing d = 90 nm and 100 nm, respectively (Figure 3-6a). In DMF, the basal spacing increased to 145 nm and 161 nm, respectively (Figure 3-6 b).

Theoretically, the basal spacing (the average distance between the nanosheets) of isotropic phase colloids are calculated by the following equations 1,

$$d = \left(\frac{\pi D^2 L}{4}\right)^{\frac{1}{3}} \phi^{-\frac{1}{3}} \quad (2),$$

where D is the nanosheet lateral size, L is the nanosheet thickness, φ is the nanosheet concentration (vol/vol). Here, according to the DLS measurement (Figure 3-7b), D = 4300 nm, while L = 1.4 nm based on the crystallographic structure. The calculated theoretical lines and experimental values of water and DMF systems is shown as the Fig. 3-7. Although the experimental values are obviously smaller than the theoretical values, this is explained by the size polydispersity of the nanosheets that leads to large number density of the nanosheets. It is notable that the DMF dispersion shows larger d than water system. This is explained by much lower ionic strength in DMF due to lower dissociation

constant of salts than water that leads to larger electric double layer repulsion between the nanosheets.

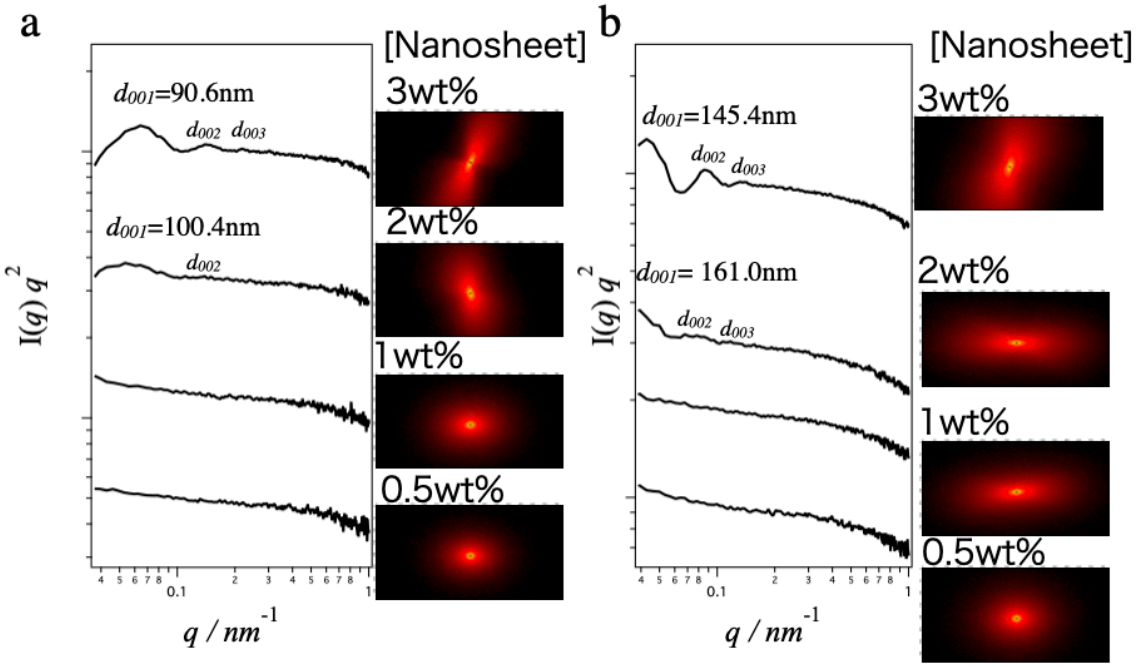

Figure 3- 6 SAXS patterns of MPDMS modified nanosheet dispersed in (a) water and (b) DMF.

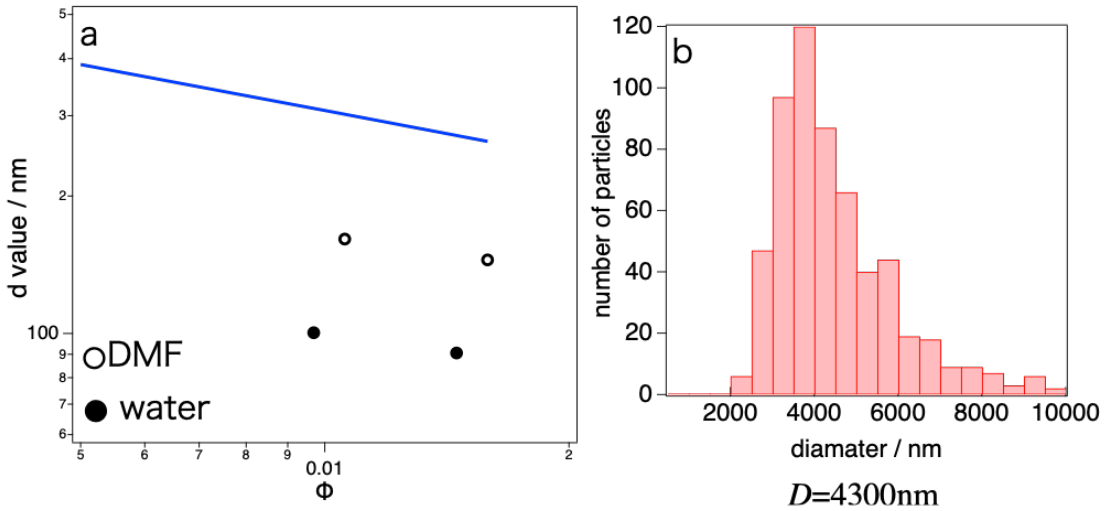

Fig.3-7 (a) The relationship between the d value and the concentration of the MPDMS modified nanosheets dispersed in DMF (open plot) and water (DMF). The solid blue line shows the theoretical line calculated for isotropic colloidal dispersion. (b) shows the diameter distribution of MPDMS grafted nanosheets measured by DLS.

Finally, further modification of the MPDMS-modified nanosheet with PMMA was successful by surface initiated radical polymerization by taking advantage of the MPDMS-modified nanosheet that is dispersed as single-layer nanosheets in DMF. AFM image of PMMA-modified nanosheet is shown in Figure 3-8. PMMA modified nanosheet had lateral size of several μm and this is mostly same as before modification. The thickness was ca. 3 nm (Figure 3-8b) that is larger than before modification (ca. 2 nm). Notably, small domains with the thickness of ca 2 nm were observed on the PMMA-modified nanosheets. These domains are the probably due to grafted polymer chains. The WAXS measurements of dried powder samples also confirmed the modification of PMMA (Figure 3-9). The basal spacing of PMMA modified nanosheet was d = 3.07 nm, that is larger than that of MPDMS modified nanosheet (2.35 nm). This increase in d-value is explained by the presence of PMMA.

Dispersibility in organic solvent was improved after grafting with PMMA-grafted nanosheets. Figure 3-10 shows the 0.1 wt% nanosheet samples with and without modification dispersed in DMF and DMF/toluene mixture (1:9 in volume) as observed with crossed polarizers (Figure 3-9). PMMA-grafted nanosheet was dispersed without aggregation and showed permanent birefringence both in DMF and mixture of DMF and toluene. In contrast, MPDMS grafted nanosheet is dispersed and shows permanent birefringence in DMF but not in DMF/toluene mixture. Nanosheet without modification is not dispersed in DMF nor in DMF/toluene mixture. The improved dispersibility is explained by steric stabilization effect of the grafted polymer chains, again confirming successful modification of PMMA.

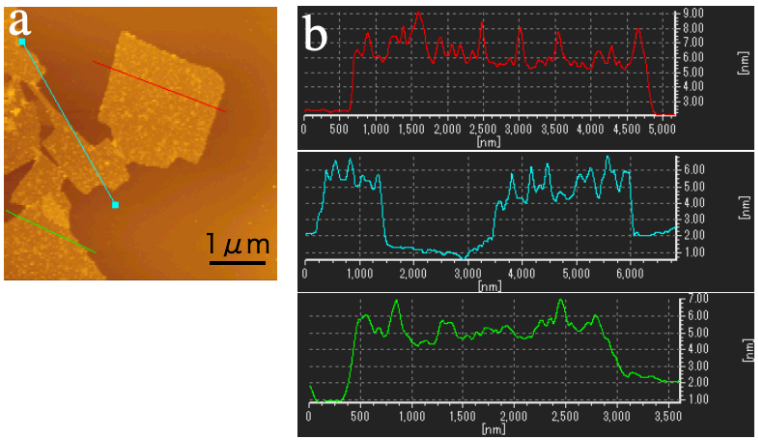

Figure 3- 8 AFM image of (a) the PMMA grafted hexaniobate nanosheet and (b) its cross section profile.

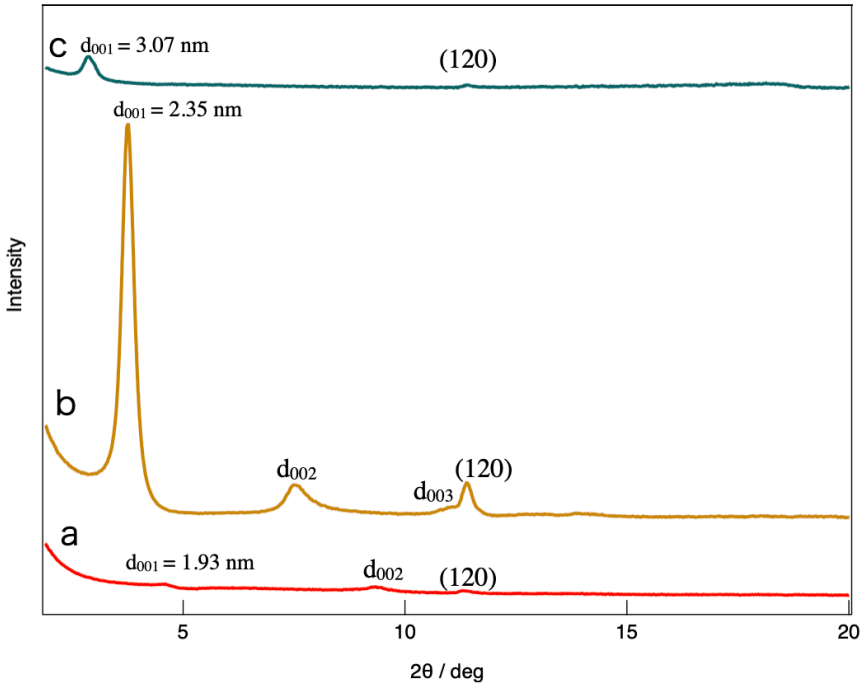

Figure 3-9 XRD patterns of the powder samples of (a) the hexaniobate nanosheets before modification, (b) MPDMS-modified nanosheet reacted for 3 days at 100 ℃, (c) and PMMA-grafted nanosheets.

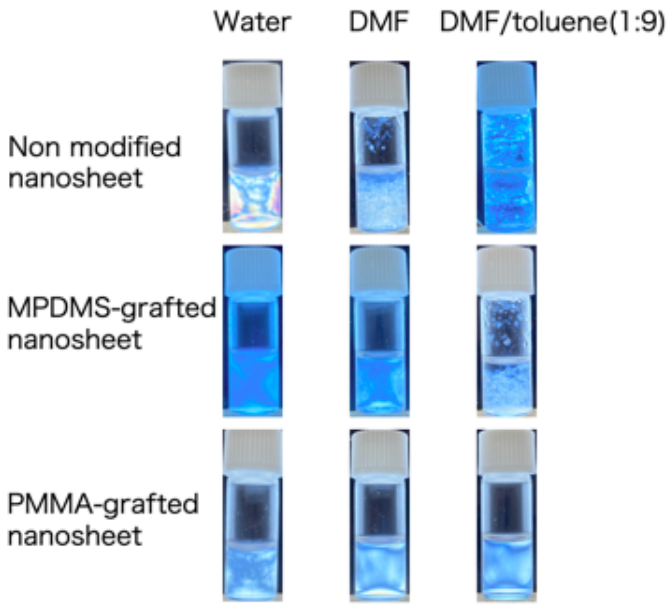

Figure 3-10 Crossed polarizer observations of the nanosheet samples dispersed in the solvents.

3.4 Conclusion

We succeeded in surface modification of single-layer niobate nanosheets dispersed in DMF/water mixture maintaining for the first time. MPDMS modified nanosheet dispersed in DMF as well as in water formed liquid crystal phase with birefringence. Furthermore, MMA was polymerized from the PMDMS modified nanosheet surface so that the obtained PMMA-nanosheet was dispersed in DMF/toluene mixture. This system will be applicable for fabrication of wide range of polymer/nanosheet composites.

3.5 Reference

1. Iijima, M.; Kobayakawa, M.; Kamiya, H., Tuning the stability of TiO2 nanoparticles in various solvents by mixed silane alkoxides. *J Colloid Interface Sci* **2009,** *337* (1), 61-5.

2. Wu, T.; Zhang, Y.; Wang, X.; Liu, S., Fabrication of Hybrid Silica Nanoparticles Densely Grafted with Thermoresponsive Poly(N-isopropylacrylamide) Brushes of Controlled Thickness via Surface-Initiated Atom Transfer Radical

Polymerization. *Chem. Mater.* **2008,** *20*, 101-109.

3. Miyamoto, N.; Nakato, T., Liquid crystalline nature of $K_4Nb_6O_{17}$ nanosheet sols and their macroscopic alignment. *Adv. Mater.* **2002,** *14* (18), 1267-1270.

4. Ide, Y.; Iwasaki, S.; Ogawa, M., Molecular recognition of 4-nonylphenol on a layered silicate modified with organic functionalities. *Langmuir* **2011,** *27* (6), 2522-7.

5. Takahashi, N.; Hata, H.; Kuroda, K., Exfoliation of Layered Silicates through Immobilization of Imidazolium Groups. *Chemistry of Materials* **2011,** *23* (2), 266-273.

6. Suzuki, R.; Sudo, M.; Hirano, M.; Idota, N.; Kunitake, M.; Nishimi, T.; Sugahara, Y., Inorganic Janus nanosheets bearing two types of covalently bound organophosphonate groups via regioselective surface modification of K4Nb6O17.3H2O. *Chem Commun (Camb)* **2018,** *54* (45), 5756-5759.

7. Ohno, K.; Zhao, C.; Nishina, Y., Polymer-Brush-Decorated Graphene Oxide: Precision Synthesis and Liquid-Crystal Formation. *Langmuir* **2019,** *35* (33), 10900-10909.

8. Chi, Z.; Zhang, X.; Xu, B.; Zhou, X.; Ma, C.; Zhang, Y.; Liu, S.; Xu, J., Recent advances in organic mechanofluorochromic materials. *Chem Soc Rev* **2012,** *41* (10), 3878-96.

9. Lomeda, J. R.; Doyle, C. D.; Kosynkin, D. V.; Hwang, W.-F.; Tour, J. M., Diazonium Functionalization of Surfactant-Wrapped Chemically Converted Graphene Sheets. *J. Am. Chem. Soc.* **2008,** *130*, 16201-16206.

10. Kimura, N.; Kato, Y.; Suzuki, R.; Shimada, A.; Tahara, S.; Nakato, T.; Matsukawa, K.; Mutin, P. H.; Sugahara, Y., Single- and double-layered organically modified nanosheets by selective interlayer grafting and exfoliation of layered potassium hexaniobate. *Langmuir* **2014,** *30* (4), 1169-75.

11. Kim, D.; Ko, T. Y.; Kim, H.; Lee, G. H.; Cho, S.; Koo, C. M., Nonpolar Organic Dispersion of 2D Ti3C2Tx MXene Flakes via Simultaneous Interfacial Chemical Grafting and Phase Transfer Method. *ACS Nano* **2019,** *13* (12), 13818-13828.

Chapter 4

Conclusion

4.1 **Conclusion**

In this study, we proposed a new surface modification method for nanosheets using hexaniobate nanosheet colloids, and succeeded in modifying the biomolecules ssDNA and PMMA.

Surface modification to the surface of nanosheets has been performed for a long time, but modification of biomolecules such as DNA and cellulose and functional molecules such as macromolecules has not been reported yet, and the modification of ssDNA and PMMA this time is important. I think it is a good result. The modification of ssDNA was carried out for the purpose of controlling nanosheets using DNA, and as the first step, ssDNA was modified on the surface of hexaniobate nanosheets via covalent bonds. Furthermore, by adding ssDNA with a base sequence complementary to the modified ssDNA on the surface of the nanosheet, it can be confirmed that hybridization is also performed on the surface of the nanosheet, which is important as a basic experiment for application as a nanocomposite material of nanosheet and DNA. It will be.

On the other hand, the modification of PMMA has obtained important results that the nanosheets can be silylated while maintaining the dispersed state in the solution. Since the conventional intercalation method and the method using the liquid-liquid two-phase system cannot be obtained in a state where the nanosheet is completely peeled off, the optical characteristics of the nanosheet colloid have not been exhibited. With this method, the nanosheets can be easily redispersed and dispersed in other solvents. Further, if other silane coupling agents can be dissolved in the mixed solvent, the surface can be modified. Furthermore, further application is possible if not only hexaniobate nanosheets but also other nanosheet colloids can be dispersed in a mixed solvent.

4.2 Publication list

"Grafting of Fluorescence-Labeled ssDNA onto Inorganic Nanosheets and Detection of a Target DNA , "

Chemistry letter (accepted for publication)

Shinya Anraku, Yoshiro Kaneko, Nobuyoshi Miyamoto.

4.3 Acknowledgments

I would like to express my gratitude to my supervisor, Professor Nobuyoshi Miyamoto, for his valuable discussion, helpful advice and continuous encouragement. I would like to express my gratitude to my supervisor, Prof. Yoshiro Kaneko, Prof. Yutaka Ohsedo, Dr. Kosuke Kaneko and Dr. Yoshihiro Nono for their valuable discussion, helpful advice and continuous encouragement. I thank to Professor Hajime Mita for his valuable discussion, suggestion and encouragement. I'm deeply grateful to Professor Wu Xing-Zheng and Professor Hiroyuki Fujioka for advice.

I thank to members of Miyamoto laboratory were also acknowledged. I especially thank to my seniors and colleagues, Dr. Shinya Yamamoto, Mr. Takumi Inadomi and Dr. Riki Kato for their continuous encouragement and giving me joy. Finally, I would like to express my gratitude to my family for financially supports, continuous encouragement and love.